HETEK

Control of Early Age Cracking in Concrete Phase 4 and 5: Material Modelling – Continuum Approach

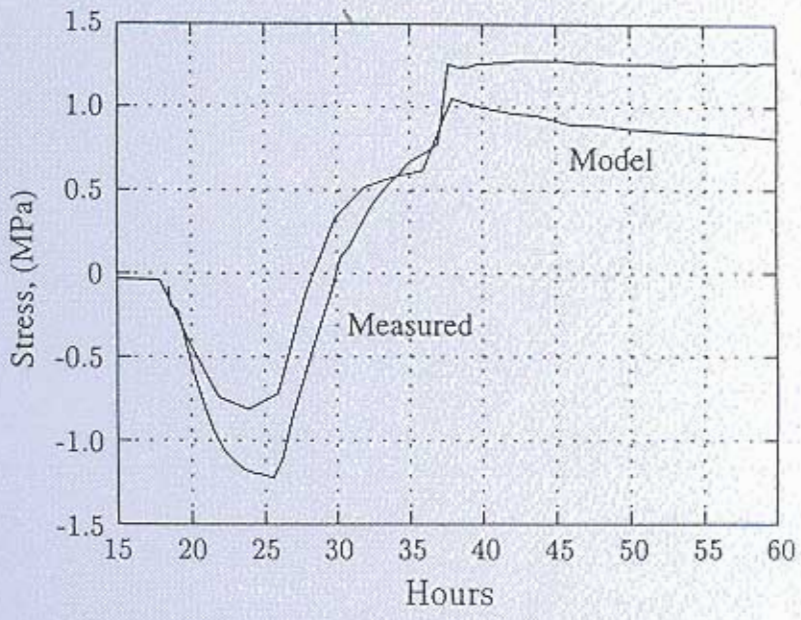

Report No.113
1997

Road Directorate Denmark Ministry of Transport

IRRD Information

Title in English	**HETEK -Control of Early Age Cracking in Concrete - Phase 4 and 5: Material Modelling, Continuum Approach**
Title in Danish	**HETEK -Styring af revner i ung beton - Fase 4 og 5: Materiale modellering baseret på en kontinuum mekanisk beskrivelse**
Authors	Anders Boe Hauggaard, Lars Damkilde, Per Freiesleben Hansen, Erik Steen Pedersen and Anders Nielsen
Subject classification	Field 32 Concrete

Key words

Concrete	4755
Analysis	7152
Material (constr)	4555
Numerical	6432
Properties	5925
Thermal stress in material	5575
Denmark	8028

Abstract

This report deals with numerical modelling of early age concrete. The hydration proces giving the strength and stiffness development after casting is discussed. Several factors influence the progress of hydration such as the temperature level and the moisture activity. The factors are coupled and a material model is proposed which include some of the couplings. It is shown how more factors may be incorporated. The model is illustrated through analysis of measured creep response both at a varying load history and at a varying temperature history.

UDK 691.32
620.191.33

ISSN 0909-4288

ISBN 87-7491-826-5

Contents

Preface

This project on control of early age cracking is a part of the Danish Road Directorates research program, High Performance Concrete – The Contractors Technology, [1] abbreviated to HETEK.

In this program high performance concrete is defined as concrete with a service life in excess of 100 years in an aggressive environment.

The research program includes investigations concerning the contractors design of high performance concrete and execution of the concrete work with reference to the required service life of 100 years.

The total HETEK research program is divided into segment parts with the following topics:

- chloride penetration
- frost resistance
- control of early age cracking
- compaction
- curing, evaporation protection
- trial casting
- repair of defects

The Danish Road Directorate invited tenders for this research program which is mainly financed by the Danish Ministry for Commerce and Industry – The Commision of Research and Development Contracts.

The present report refers to the part of the HETEK project which deals with control of early age cracking.

For Durability reasons reinforced structural members should be well protected against penetration of water, chloride etc. This means that cracks should be avoided or at least the crack-width limited. Formation of cracks can take place already during the hardening process. An evaluation of the risk of crack formation involves a stress analysis. In stress analysis of hardening concrete structures, the load consists of the difference in thermal strains that arise from the heat of hydration. The mechanical properties, including autogenous shrinkage, of the concrete also change during the hardening process. If a stress analysis shows high stresses compared to the tensile strength there is a high risk of crack formation.

The purpose of this project is to investigate these effects and to prepare a guideline regarding Control of Early Age Cracking.

The project was carried out by a consortium consisting of:

Danish Concrete Institute represented by:

[1] In Danish: Højkvalitetsbeton – Entreprenørens Teknologi

- Højgaard & Schultz A/S
- Monberg & Thorsen A/S
- Rambøll
- COWI

and Danish Technological Institute, represented by the Concrete Center and Technical University of Denmark, represented by the Department of Structural Engineering and Materials.

Two external consultants, Professor Per Freiesleben Hansen and manager Jens Frandsen, are connected with the consortium.

The present part of the HETEK project, Material Modelling, Continuum Approach, is carried out at the Technical University of Denmark. The report covers the originally phase 4 "Material Modelling" and phase 5 "Documentation of Model, Test Frame".

Chapter 1

Introduction

1.1 Numerical Modelling of Early Age Concrete

A numerical analysis of strains and stresses in a concrete structure in the early age after casting has several purposes, such as

- predict the risk for harmful cracking
- planning of the formwork arrangement
- predicting of the time at which the formwork may be removed
- considering the influence of seasonal conditions, e.g. winter concreting

Generally the formwork may be removed when the concrete can carry its own weight. From the numerical analysis the temperature and maturity development in time is known and thus removal of formwork may take place when the temperature and temperature profile has reached a value corresponding to a sufficient value of the maturity for formwork removal. The newly cast concrete exerts pressure on the formwork and the variation in time of this pressure may be used to determine when it is safe to release the tightening or remove the forms.

Normally formwork is removed, when the concrete has a given maturity, [20] and [21], and thus a given strength. An alternative criteria for formwork removal may be that the immediate cooling of the surface gives no risk of formation of thermal cracking. This means that the temperature is used as control parameter in the early age. This may be advantageous since it is easy to measure the temperature continously, [23].

Normally a separation is made in the assessment of cracking between

- no cracking in the structure
- control on the width of the cracks in the structure

In areas subjected to harsh environments, such as the splash-zone of off-shore structures or where the concrete is subjected to deicing salts, it is preferable to avoid cracking while it

suffices in other areas to control the crackwidth. Emphasis on cracking is due to the close relation between permeability and durability, e.g. in connection to

- penetration of chlorides and corrosion,
- damage due to freezing
- sulphate attack

Criterias for crack formation are not trivial and a possible criteria is related to the tension strength of the concrete. After initiation of cracking, stresses are still transfered over the cracking plane, [30], and this influences the statical behaviour of the structure.

Different structural systems may be analysed numerically during the design work. This has special interest in relation to large concrete works were little experience is available e.g. due to complicated geometrical shapes. Further different arrangements of cooling or heating pipes may be compared before casting.

In the assessment of the early ages criterias based on the maximum temperature difference within the structure are normally used, [58]. But these types of criterias have shown to be insufficient in situations where stresses gradually are being build up, e.g. when larger structures are cast [17], [2] and [42], and therefore an analysis of the stress development at early ages is needed. A limitation of the criterias based on temperature differences is that the same temperature history generates different stresses depending on the restraints. However for smaller structures where chock cooling is taking place the temperature criterias suffices.

The measures which are used for the numerical analysis are

- the maturity development
- the temperature development
- the development of the moisture distribution
- the development of stresses

The variation in time of these measures is determined by the hydration process, which is the exothermic reactions between cement and water. The hydration process stops when all the free capillary water is combined in the formed hydrates, e.g. [6], and therefore the moisture distribution influences the early ages of a concrete structure. This situation is in particularly of importance in relation to modern concretes with low water/cement ratios and low permeability, meaning that the moisture supply from the environment is slow. Therefore the concrete may dry up internally and the hydration process cease, this phenomenon is termed self-dessication, [31] and [32].

The development of the maturity and the temperature are interrelated and this subject is discussed later. The effects of importance at early ages are coupled, e.g. the heat development from the hydration process accelerates the hydration process and thereby increases the rate of heat development, [18].

A restrained structure in which the temperature or moisture distribution changes may crack due to the stresses generated from the differential strains. The structure may be restrained by adjoining structures or internally due to the aggregate. The magnitude of the strains following a change in temperature or moisture distribution depends on the thermal expansion and the shrinkage parameters. During the heating period the stiffness is low and this means that the stresses generated are relatively low. However surface cracking is seen in this period due to that the center of the structure becomes varmer than the surface. In the subsequent cooling period when the stiffness has increased the stress changes are larger and through cracks may appear, [17].

The numerical methods used in the analysis of the properties of hardening concrete are based on the finite element concept and different programs are available, e.g. CIMS-2D, [15], Fiesta, [22], DIANA, [10], COSMOS, [16], LUSAS, [36] and HACON-S, [56]. The programs have some limitations e.g. in relation to

- the development in time of the material properties
- the incorporation of the couplings

Some of the programs describe the development of the material parameters in time with mathematical expressions having no relation to the underlying physical processes, e.g. [8]. Furthermore the couplings between effects lack sufficient generality. This means that some effects are not included at all or they are treated insufficiently. For a realistic modelling of the stress development there is a need for material models based on the physical process at early ages.

1.2 Features of a Numerical Method

An analysis with finite elements is based on

- a material model for calculating the development of strains and stresses, including a crack model
- the temperature development
- the development of the moisture distribution

In the analysis with finite elements the structure is subdivided into elements. The changes of e.g. temperature are spreading through adjoining elements, as shown in Fig. 1.1. Here heating of element 3 has propagated to the adjoining elements. The structure shown in Fig. 1.1 is supported along two sides and this causes stresses mainly along the supports, i.e. the heating initially gives compressive stresses in the structure here and upon the subsequent cooling the stresses are reversed into tension. The material model need to include this development in time of the material properties, and effects from e.g. the thermal and shrinkage strains.

The existing programs are able to predict the temperature development with sufficient accuracy for practical purposes, e.g. the accuracy of the temperatures determined with the

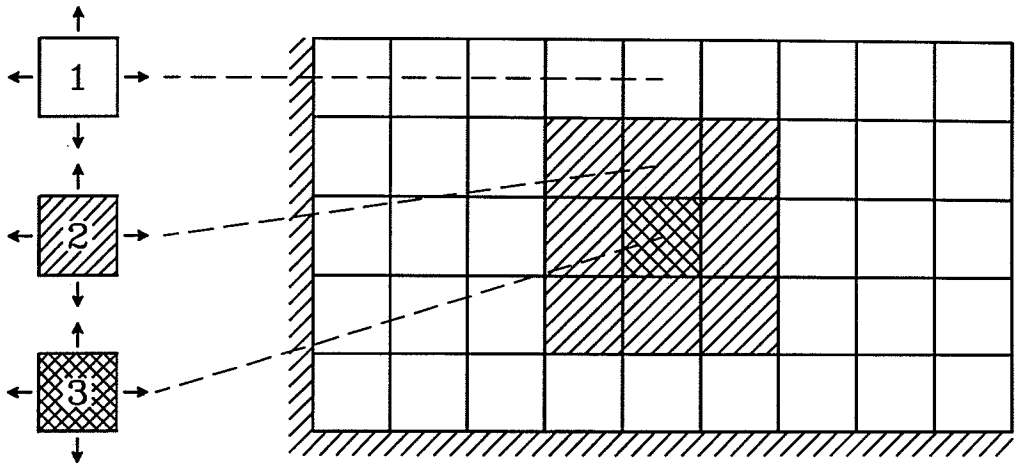

Figure 1.1: Interaction between finite elements.

program CIMS-2D are within 2-3°C. However, at present none of the programs mentioned above include the effect of the moisture content on the hydration processes. This may be of importance when analysing the situation after formwork removal where the structure is subjected to the environmental humidity.

The variation of the shrinkage strains may be obtained from experimental observations or by using calculated moisture distributions in the structure. Experimentally, it has been found that the shrinkage strains are almost proportional to the moisture loss, [14]. However this result apply only to concrete cured for one month or more. The modelling of shrinkage at early ages is the scope in [28] and here it is found that the shrinkage strains at early age may offset the temperature strains in the heating period and result in tensile stresses and thus cracking. This result apply for high strength concrete with a water to cement ratio below about 0.34. The driving potential in the shrinkage is the changes in the moisture distribution, but shrinkage modelling is outside the scope of this work.

Chapter 2

Material Models

The purpose of a material model is to describe the behaviour of a structure or measurements made in the laboratory on a test specimen. In the formulation of the model assumptions are introduced about the material, e.g.

- which effects are incorporated
- how are the couplings included

The assumptions define the limitations of the model and the scope is to make the model sufficient for the actual problem and make sure that the computational effort is acceptable. The concept chosen for numerical material modelling is normally either the total or the incremental one and below both types are summerised. Further the model chosen in CIMS-2D is outlined. The concepts are illustrated with creep models as example.

2.1 Standard Creep Models

The principle of creep modelling normally used may be illustrated with the classical aging viscoelastic models, [6]. The models are based on the assumption that alle sorts of loading may be predicted, such as stress, temperature and humidity variations throughout the lifetime of the structure. That is the complete loading history, $\boldsymbol{\sigma}(t)$, is needed. An example on the viscoelastic models is

$$\varepsilon(t) = \int_0^t J(t,\tau)\boldsymbol{D}d\boldsymbol{\sigma}(\tau) + \varepsilon_0(t) \tag{2.1}$$

from [6], where ε are the strains at time t, J is the compliance function, τ is the time at loading, $\boldsymbol{D}$ is a constant matrix given by Poissons ratio and used for generalisation to multi-dimensional cases and $\boldsymbol{\sigma}$ is the stresses. All sorts of strains without relation to the stresses are given by ε_0, and contributions come from e.g. thermal deformations or shrinkage. (2.1) is a relation between the actual total strains, ε, and the loading history and therefore the model is termed a total model.

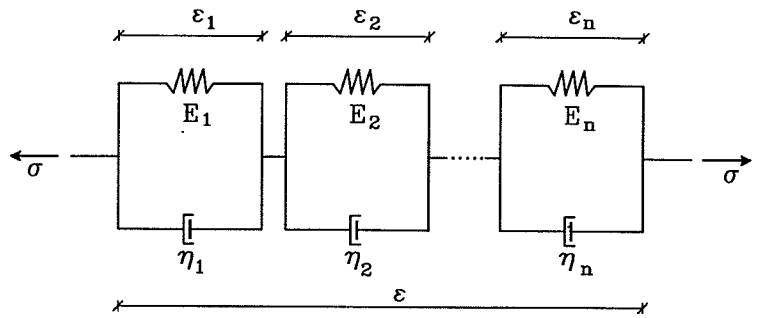

Figure 2.1: The rheologic model obtained as a result of the expansion of the compliance function.

The purpose of (2.1) is to determine the variation of strains with time for an arbitrary stress historie. This is done based on the compliance function and the complete stress history, $\boldsymbol{\sigma}$. The material properties are given by the compliance function and this include effects from change of temperature and moisture distribution. Normally the compliance function is obtained by fitting experimental data with empirical relations, [6].

In a numerical analysis (2.1) is inconvenient because at each time

- computation of sums with many terms are needed
- the complete stress history need to be stored

To avoid these shortcommings an expansion of the compliance function, J, is made before a numerical analysis is done, e.g. as in the program DIANA described in [11] or as shown in [6], and hereby transforming (2.1) to an expression of the form

$$\varepsilon(t) = \Sigma_{i=1}^{n} \varepsilon_i(t) + \varepsilon_0(t) \tag{2.2}$$

where n is the number of terms in the expansion and ε_i is the contribution from the i'th term. The contribution $\varepsilon_0(t)$ in (2.2) incorporate all sorts of strains which do not depend on mechanical load, such as thermal and shrinkage strains. Each term in the sum in (2.2) may be interpreted as the strain in a Kelvin cell as shown in Fig. 2.1.

The parameters in Fig. 2.1, the modulus of elasticity, $E_i(t)$, and the viscosities, $\eta_i(t)$, are obtained from the expansion and they are functions of time. Since the expansion is a mathematical tool it is uncertain whether the parameters are physical realistic. This may lead to inconsistencies, such as a decreasing elastic modulus during the hardening process in one of the Kelvin cells, [6]. Therefore it is difficult to relate the coefficients in the rheologic model to the proceeding of the hydration process.

The expansion of the compliance function is used to formulate a model suitable for implementation in a finite element code, and this model is termed an incremental model, e.g. [6]. In the incremental formulation the history is included using variables which are summed during the calculation. These variables for the aging viscoelastic models are the strains in the individual cells, ε_i, shown in Fig. 2.1.

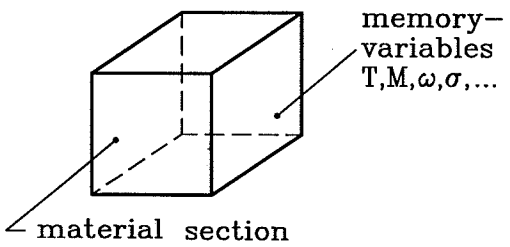

Figure 2.2: Memory-variables.

The procedure when using a total viscoelastic model is summerised in the following three steps

- obtain the compliance function, empirically or theoretically
- expand the compliance function to obtain the rheologic model
- establish the incremental form

The influence from temperature and moisture effects are normally included using factors on the coefficients, e.g. as shown for changes in the moisture distributions in [9].

2.2 Incremental Material Modelling

Since the incremental type of material models is used as basis later, we discuss the concept more in detail here. The discussion includes

- memory-variables
- a linearisation of the properties

The assumption when using the incremental models is that the material has a limited memory and therefore the behavior may be characterised with certain variables termed the memory variables. These variables are used in the model as shown in Fig. 2.2 where the behaviour is given by the temperature, T, the stresses, $\boldsymbol{\sigma}$, the moisture content, w, and the maturity age, M. Thermodynamic considerations may be used to give an idea of what could enter as a memory variable, [5] and [27]. The above values are rather simple memory-variables as they are given by the actual state of the material section.

For inclusion of the memory, e.g. in connection to the loading history, memory variables of the form

$$L(t) = \int_0^t u\sigma dt \tag{2.3}$$

may be used. In (2.3) the stresses, σ, have been weighted with the function u and integrated through time, t, to the memory-variable L. The idea is to use L in the material description.

In this way influence from stresses on the structure of the hydration products, [38], is included using a relative large weight for early stresses. The modulus of elasticity from standard tests are normally slightly lower than the modulus of elasticity obtained from creep experiments and this indicate some influence from the loading on the properties.

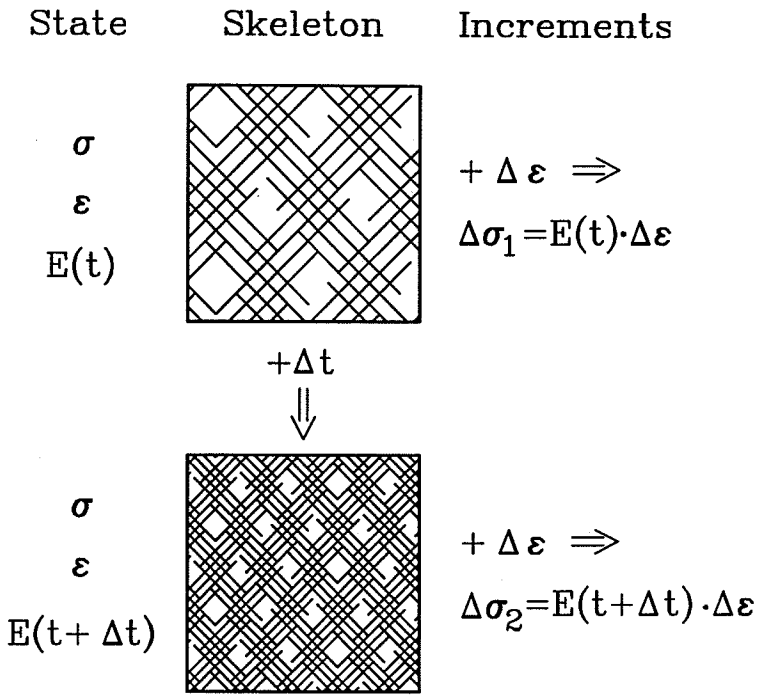

Figure 2.3: Influence from time and loading on an aging material.

The response of an aging material without any viscoelastic effects to time and load is illustrated in Fig. 2.3. Initially the state of the material is characterised with the memory-variables stress, $\boldsymbol{\sigma}$, strains ,$\boldsymbol{\varepsilon}$, and the value of the modulus of elasticity, $E(t)$, at time t. A time-step, Δt, later more reaction products have been formed as shown with the more dense filling and this results in an increase of the elastic modulus to $E(t + \Delta t)$. However the stresses and strains remains unchanged since viscoelastic effects are disregarded. Application of a strain change, $\Delta\boldsymbol{\varepsilon}$, at time t results in the stress change, $\Delta\boldsymbol{\sigma}_1$, that depends on the actual value of the elastic modulus. Later application of the same strain change results in a different stress change $\Delta\boldsymbol{\sigma}_2$ due to the increased value of the elastic modulus. This leads to a linearisation of the properties where the relation between stresses and strains, the constitutive equation, is given in increments

$$\dot{\boldsymbol{\sigma}} = \boldsymbol{D}_t\dot{\boldsymbol{\varepsilon}} \tag{2.4}$$

The form of the constitutive equation, (2.4), has been analysed in [6] using thermodynamics and it was found that it is the only possible one for an aging material not violating thermodynamical requirements.

The matrix, $\boldsymbol{D}_t$, is the constitutive matrix and t emphasises that it represents a linearisation of the properties as shown in Fig. 2.4 for the one-dimensional case.

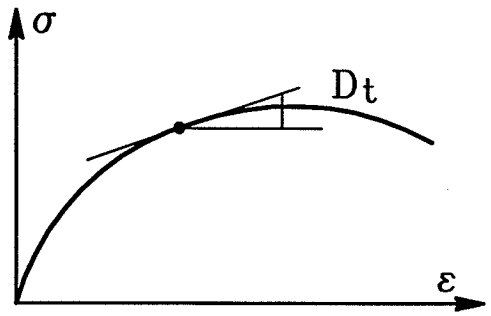

Figure 2.4: Tangent relation between stress and strain.

Using an incremental formulation as basis for the material modelling makes the model readily suited for implementation in a finite element context. In the incremental material model the constitutive matrix is written as a function of the memory-variables

$$\boldsymbol{D}_t = \boldsymbol{D}_t(T, h, M, w, L, \ldots) \tag{2.5}$$

The principle is to take as basis a rheologic model and fit experimental data directly without the intermediate step with the compliance function, e.g. as described in [27]. In the fitting process the variation in time of the parameters in the rheologic model is determined. Then the rheologic model is used in the numerical analysis for determining the variation of stresses and strains and following this procedure the inconsistencies mentioned in relation to the total models are avoided.

Equilibrium in the incremental viscoelastic models are formulated in incremental form, e.g. as shown in [27]. Based on one cell of the model shown in Fig. 2.1 the stress increment is

$$\dot{\sigma} = \dot{\sigma}_s + \dot{\sigma}_d \tag{2.6}$$

where $\dot{\sigma}_s$ is the stress increment in the spring written

$$\dot{\sigma}_s = E_i(t) \cdot \dot{\varepsilon}_i \tag{2.7}$$

and $\dot{\sigma}_d$ is the stress increment in the dash-pot written

$$\dot{\sigma}_d = \dot{\eta}_i(t) \cdot \dot{\varepsilon}_i + \eta_i(t) \cdot \ddot{\varepsilon}_i \tag{2.8}$$

In the incremental forms the variation of the properties in time are considered.

In excess of the influence from the memory-variables on the hydration process they also influence the structure of the hydration products, [48], and thereby the mechanical behaviour of the concrete. Further relations between the memory-variables and e.g. creep properties and strength have been reported from several experiments.

Chapter 3

Early Age Concrete

3.1 The Chemical Reactions

Concrete is a composit material and the constituents are

- capillary water
- adsorbed water
- unhydrated cement particles
- cement gel
- aggregate
- additives such as fly ash, microsilica or chemical admixtures

In the numerical approach chosen here concrete is treated as a homogeneous material and therefore average stresses are calculated. This means that the stresses are not usable in e.g. the boundary zones around aggregate. The stresses may be used only for regions with a size larger than some characteristic dimension, e.g. related to the maximum aggregate size.

Another approach is the composite theory and this has been used where the aggregate consists of fibers or other well-defined inclusions, e.g. in relation to ceramics and polymers. In [40] it was used in relation to concrete and the material was considered as a multi-phase system where aggregate is distributed in a homogeneous cement paste. The effect of adding fibers to hardened concrete was studied experimentally in [35] and the tensile behavior observed was explained using the composite approach. In our application we believe that this approach is too detailed for several reasons, such as

- non-uniform stress-distribution around the aggregates
- the shape of the aggregates
- the size distribution of aggregate

- the distribution of aggregate in the cement paste
- incomplete adhesion between aggregate and cement paste
- the development of the properties in time

The stresses around general shaped aggregates is complicated and a solution based on well-defined particles may be far from the correct one. The size of the aggregate is varying over several decades and the location of the various aggregates in the paste is unknown. Further the adhesion between aggregate and cement paste is not complete, [37], causing deviations which are difficult to measure and control. In excess of this the properties develop in time and e.g. the behavior of the interface zone between aggregate and cement paste may change significantly.

The cement gel is the product from the hydration process between cement and water, and the gradual increase in the amount of formed cement gel is the main reason for the change of the concrete properties at early ages.

The constituents of the cement particles are mainly the four minerals tricalcium silicate, $3CaO \cdot SiO_2$, dicalcium silicate, $2CaO \cdot SiO_2$, tricalcium aluminate, $3CaO \cdot Al_2O_3$, and tetracalcium alumino ferrite, $4CaO \cdot Al_2O_3 \cdot Fe_2O_3$, and therefore separation is made between at least four chemical reactions, [18] og [13]. The reactions are developing different in time and thus the contribution to e.g. the strength and heat development from the reactions are different.

A weighted average of the reactions is termed the hydration process and Fig. 3.1 shows the terminology for a cement particle.

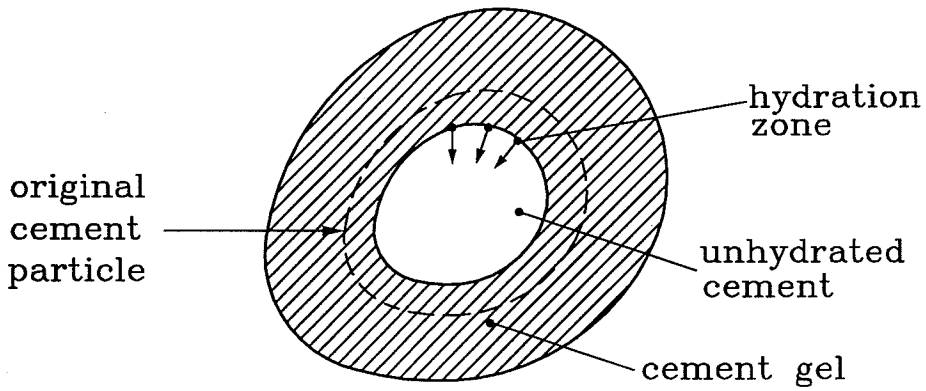

Figure 3.1: Principle sketch of the hydration process.

A separation is made between the zones with

- unhydrated cement
- hydration reaction
- hydrated cement, the cement gel

The hydration takes place on the surface of the unhydrated cement particle and the progress of the reactions is normally described using the dimensionless parameter, α, termed the degree of hydration. The degree of hydration is the ratio of cement reacted to the original amount of cement, [18]. Various methods exist to measure the quantities needed for calculating the degree of hydration, e.g. measurements of the heat developed or the amount of nonevaporable water, [13].

3.2 Couplings in Early Age Concrete

For a given concrete the progress of the hydration is determined by

- the development of the temperature
- the development of the moisture distribution

The various effects related to the hydration process are shown in Fig. 3.2 together with some of the couplings. A subdivision into three areas have been made

1. top: the environment
2. middle: the chemical reactions
3. bottom: numerical parameters

The environment includes the impact on the hydration process from other sources than what have been added when mixing, e.g. heat exchange and evaporation. This could also include the time of start of drying and size of the structure. The chemical subsection describes the reactions taking place. Finally the bottom refer to the parameters used in a numerical analysis.
The key point in the present context is the concrete properties, bottom section in Fig. 3.2, which are varying at early ages and they are subdivided into

- thermal properties
- moisture properties
- coefficient of thermal expansion and shrinkage
- stiffness and strength

The thermal properties are the thermal conductivity and the heat capacity and similarly moisture properties are the diffusion coefficient and the moisture capacity. These properties govern the development of temperature and moisture in time. The strains related to the temperature and moisture distribution in the structure are calculated using the coefficient of thermal expansion and the shrinkage coefficient. These coefficients are the

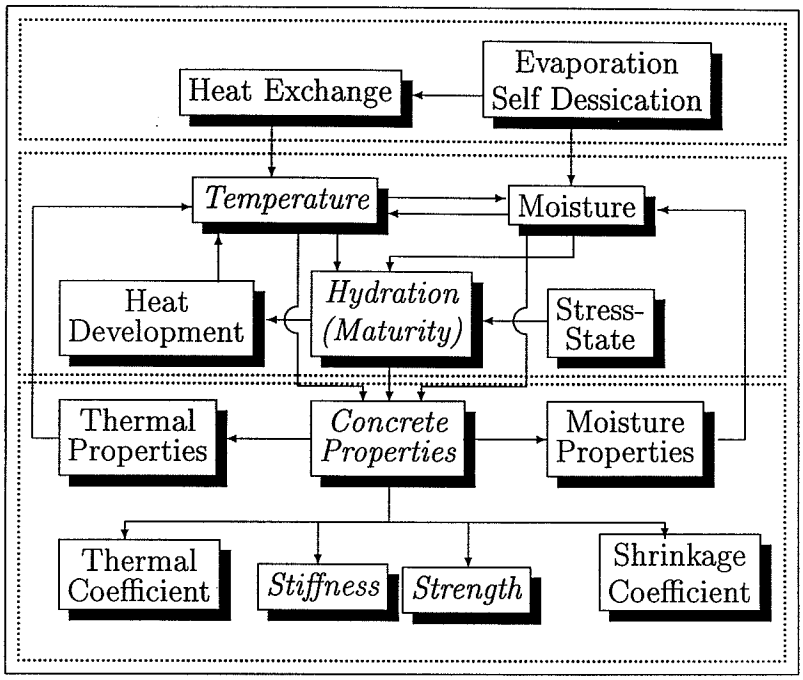

Figure 3.2: Couplings in early age concrete.

proportionality constants between change in temperature and moisture distribution, respectively, and the associated strains. Other shrinkage mechanisms also appear such as carbonation shrinkage, [38], but they are not included in Fig. 3.2.

The stiffness of the concrete is represented by the usual modulus of elasticity and the strengths are the compression and tensile strength, the latter one of importance in relation to cracking.

The change of the properties is governed by the hydration process and as other chemical reactions it depends on the temperature. In excess of this the hydration process develops heat and thus gives feedback to itself, as shown in Fig. 3.2.

Since hydration is reactions between water and cement, water is needed for the hydration process, [18] and [13]. It has been found experimentally that hydration almost ceases for relative vapor pressures below about 0.8, [45] and [41].

Generally the effects giving the temperature in the structure are

- the hydration process
- the thermal properties
- the heat exchange
- the moisture content

Water has a relatively high heat capacity, [29], and therefore diffusing moisture may transfer relative large amounts of heat. Further the heat exchange is influenced by evaporation from the surfaces of the structure. This is because a surface layer where drying takes place isolate thermally.

The development of the moisture distribution is determined by

- evaporation
- self-desiccation
- the moisture properties

Evaporation takes place when the structure is placed in an environment with a relative humidity lower than inside the concrete. Self-desiccation takes place among other when water is combined in the hydration process.

Finally some experiments indicate that the stress state influences the hydration process, [38] and [17], and this is also shown in Fig. 3.2.

In excess of the couplings mentioned in relation to Fig. 3.2 the following effects influences the hydration process, [18] and [13]

- the cementtype
- the fineness of the cement particles
- the concrete composition, the water/cement ratio
- additives, fly ash, microsilica and chemical admixtures

A mathematical description of the influence of temperature on the hydration process is normally accomplished assuming a relation of the form

$$\frac{d\alpha}{dt} = g(\alpha)f(T) \tag{3.1}$$

meaning that the rate of the hydration is separated in a function, g, of the actual degree of hydration, α, and a function, f, of temperature, T, and thus at a given degree of hydration the rate of hydration is a function of temperature only, [18].

Using (3.1) two hydration processes at different temperature histories but at the same degree of hydration may be compared and normally one of the histories is chosen as a reference history at a constant isotherm temperature of $T_0 = 20°C$. The maturity age, M, for these two processes is then given as

$$M = t_0 H(T_0) = \int_0^{t_0} \frac{f(T(t))}{f(T_0)} dt \tag{3.2}$$

and t_0 is termed the equivalent hydration period at the reference temperature and H is the rate factor $f(T(t))/f(T_0)$. After introduction of t_0 and M the hydration process becomes a function of M only, [13] and [18].

The maturity principle is based on the assumption (3.1) and thus that enough moisture is present. Further it is assumed that the structure of the formed hydration products has no influence on the hydration process as discussed before.

To include more of the factors of influence on the hydration process in the material model it may be necessary to separate the various chemical reactions. In this separation consideration may be given to the different developments in time and the different contribution to the properties of the concrete from each chemical reaction, [13].

3.3 Experimental Observations from the Literature

The result of the hydration is that the properties are developing and Fig. 3.3 and Fig. 3.4 shows two examples where the abscissas are equivalent maturity hours at a temperature $T_0 = 20°C$. Fig. 3.3 shows the development of the modulus of elasticity for a particular concrete and it is seen that about 90% of the ultimate value is reached after 4 maturity days.

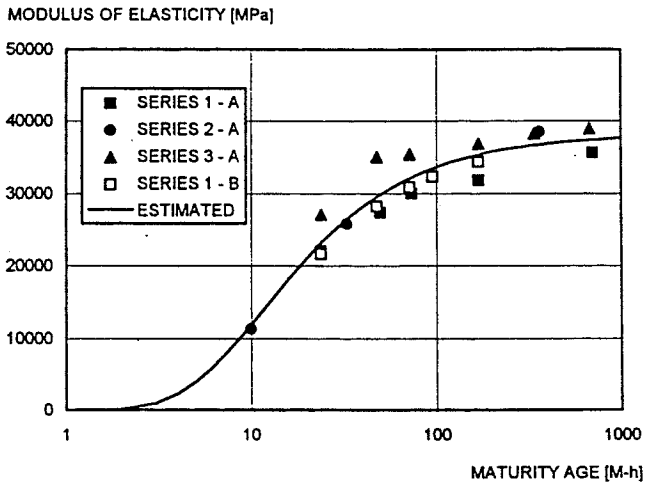

Figure 3.3: Development of the modulus of elasticity, [2].

Fig. 3.4 shows the development of the splitting strength at early ages and comparing with Fig. 3.3 it is seen that the splitting strength is increasing at a slower rate than the modulus of elasticity for this concrete. This is a general result and is also applying in relation to the compressive strength, [24].

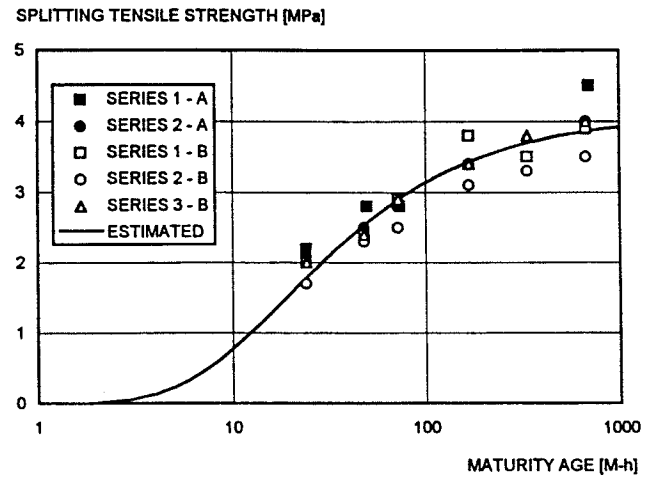

Figure 3.4: Development of the splitting strength, [2].

The development of the Poisson ratio is shown in Fig. 3.5 and it is seen that the ratio is decreasing from a value initially of 0.5 to almost zero after 10 hours and then increases to the ultimate value 0.2 at complete hydration.

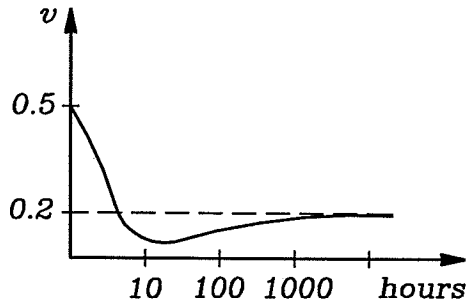

Figure 3.5: Development of the Poisson ratio, e.g. [2].

Immediately after casting the behaviour of the concrete is almost as a fluid and therefore the Poisson ratio is 0.5. In the first hours after setting the ratio undergoes large changes and this is of importance in the development of multi-dimensional stresses.

The development of the tensile strain capacity is shown in Fig. 3.6 and the similarity with the development of the Poisson ratio is remarkable, but note that the ordinate in Fig. 3.6 is logarithmic.

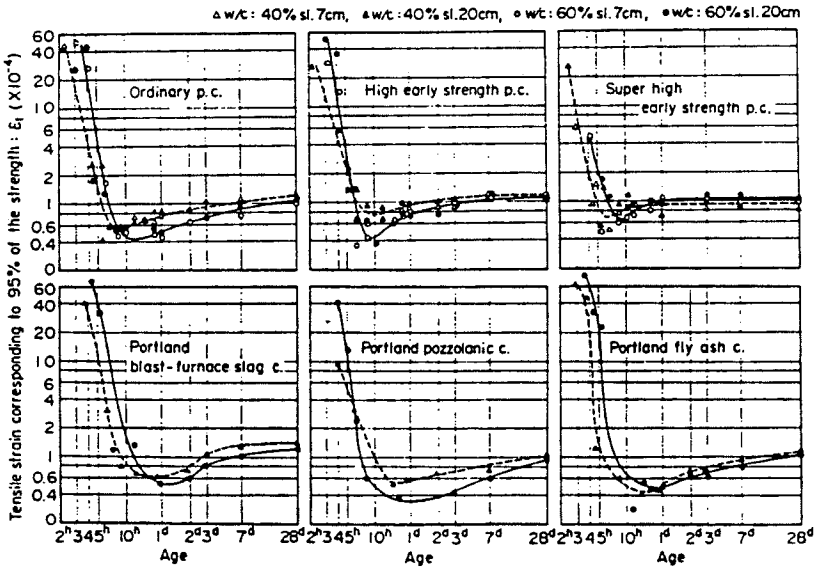

Figure 3.6: Development of tensile strain capacity, [33].

While the concrete is in the plastic state the tensile strain capacity is still relatively high and during the setting time the tensile strain capacity decreases fast almost with a factor 100. For later ages the tensile strain capacity increases with a factor 3 and the duration is about 28 days.

Couplings between creep and moisture loading are described e.g. in [43], [34], [46] and [38] and the result is shown in Fig. 3.7.

The top of Fig. 3.7 shows that creep is decreasing with decreasing constant relative humidity in the concrete, and in a complete dry concrete creep is moderate, [25]. The magnitude

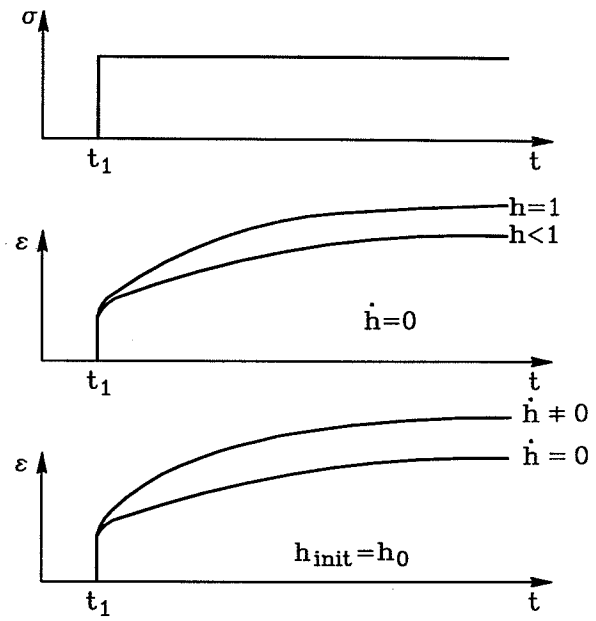

Figure 3.7: The principle relation between creep and moisture. Top: The load history. Middle: Creep history for two concretes where no exchange of moisture with the environment is taking place, $\dot{h} = 0$, one is water cured, $h = 1$, and the other has been brought to equilibrium at a lower relative humidity, $h < 1$. Bottom: Creep history for two concretes which initially have been brought to equilibrium at the same relative humidity, $h_{init} = h_0$, whereafter one of them is exchanging moisture with the environment, $\dot{h} \neq 0$, while the other is kept in equilibrium, $\dot{h} = 0$.

of creep for a saturated specimen to the magnitude of creep for a dry specimen has been reported to be approximately 5 in [39].

The bottom of Fig. 3.7 shows the creep behaviour when the concrete is exchanging moisture with the environment and for this case it is seen that creep increases both for an increase in relative humidity and for a decrease in humidity. The relation between moisture changes and creep is termed the Pickett effect because it was observed experimentally for the first time by Pickett in 1942, [43]. Typically the Pickett effect result in a magnification of the creep deformations with a factor 2-3, [9]. This correspond to a situation where sealed concrete is brought to an environment with a relative humidity of about 50% and loaded. In the present context this may be of little importance while the forms have not been removed. However, after form removal the outer layers of the concrete are subjected to the environmental humidity which may be low and then influencing the properties. The modelling of the effects related to changes in temperature and moisture distributions need to consider the different time constants in the processes. Drying of concrete may take several years while temperature equilibrium is established in a much shorter time, e.g. [6]. Temperature gradients in the concrete may also induce changes in the moisture distribution due to the dependence of the vapor pressure on temperature.

A similar behaviour has been observed for the coupling between creep and temperature

loading as shown in Fig. 3.8.

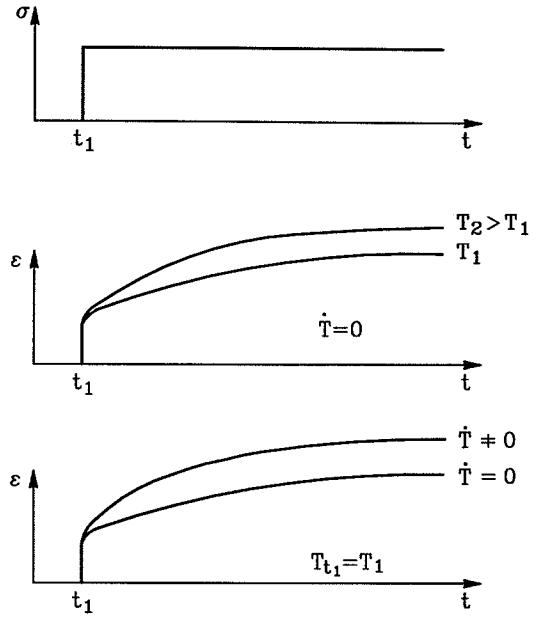

Figure 3.8: The principle relation between creep and temperature. Top: The load history. Middle: Creep history for two concretes which are in thermal equilibrium, $\dot{T} = 0$, at two different constant temperatures, T_1 respectively T_2, and $T_2 > T_1$. Bottom: Creep history for two concretes initially in equilibrium at the same temperature, $T_{t_1} = T_1$, whereafter the temperature is kept constant in one of them, $\dot{T} = 0$, while varied in the other, $\dot{T} \neq 0$.

The situation in Fig. 3.8 shows that increased constant temperature gives increased creep and that changes in temperatures also increases creep, both for increasing and decreasing temperature, [6], [17], [34], [46] and [38]. When the temperature is increased with a factor 2 the increase in creep for hardened concrete, age 15 days, is about 25%, [3]. For hardening concrete a similar result was obtained in [55] and this increase in temperature is likely to occur at early ages.

Fig. 3.9 shows the creep properties for a combined action of temperature and moisture load on the creep rate.

We are only concerned with temperatures above the freezing point and it is seen in Fig. 3.9 that for the temperature range $0°C$ up till $50°C$ the rate of creep increases with temperature both for sealed concrete and for concrete exchanging moisture with the environment. At 50 $°C$ a separation in behavior is observed and in the range $50°C$ to $100°C$ the creep rate keeps increasing for the sealed concrete whereas it decreases for the concrete exchanging moisture with the environment. When the concrete which exchanges moisture is completely dry it follows the same relation between creep rate and temperature as concrete which has previously been dried at $105°C$.

The mechanisms governing the coupling between creep, temperature and moisture is explained in [46], [4], [5] and [6] with changes in the moisture distribution in the concrete

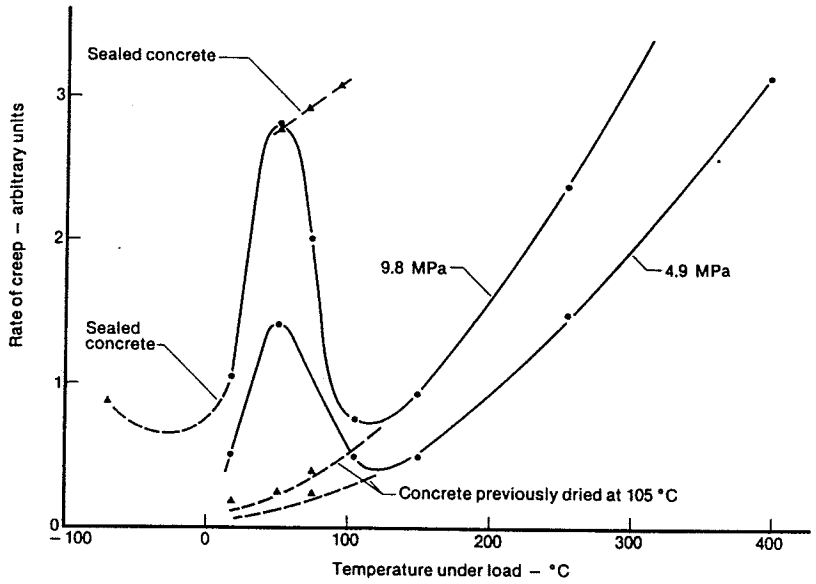

Figure 3.9: Creep, temperature og moisture, [38].

brought about by temperature and load. While the moisture distribution is changing water is transported in the microstructure of the cement gel. This increases creep because the microstructure becomes more flexible when the water carrying load is moving. At constant moisture content creep increases with the moisture content and completely dry concrete only creeps about 10% of saturated concrete, [39].

The relation between temperature and temperature changes and creep is due to the increased activity of the moisture when the temperature is either increased to a constant higher level or changing, [4], [5] og [6].

The temperature also influences the structure of the hydration products and that is explained in [48] by a fast early hydration at high temperature which gives a dense and tight structure at the surface of the cement particles. This process may explain why the long term strength decreases with increased isotherm temperature maintained during the hydration period, [13] and [19], as shown in Fig. 3.10.

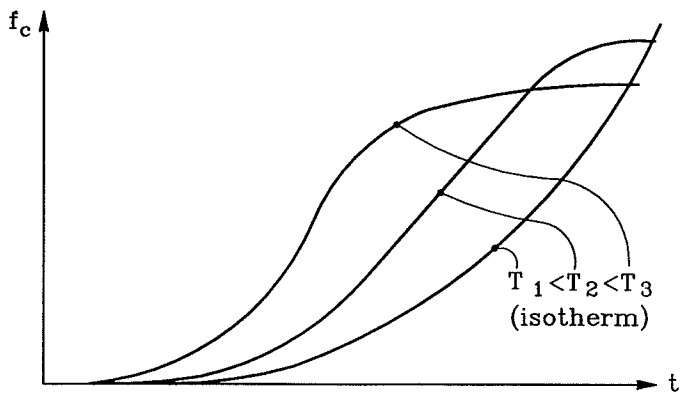

Figure 3.10: Principle development of the strength at different isotherm temperatures, note that the abscissa is logaritmic.

The dense structure at the surface changes the hydration process from chemical controlled to diffusion controlled and the diffusion of moisture into the hydration zone is slower than the chemical reaction, [48].

An increasing amount of silica fume is used in high strength concretes lowering the permeability and this means that moisture diffusion into the hydration zones is low. Therefore self-dessication may take place and in [31] the decrease in internal relative humidity due to this phenomenon has been measured to 75% and this influences both the hydration process and the creep behaviour. In excess of this self-dessication provoke shrinkage by itself.

In [44] shrinkage stresses in concrete have been measured and a coupling to the creep was found which is due to the relaxation of shrinkage stresses caused by creep. The magnitude of the shrinkage stresses also depend on the restraints of the structure. The relaxation phenomenon is a general property of creep e.g. also in connection to cracking where stress singularities are relieved by creep.

Normally a separation is made between basic- and drying creep, e.g. [25], [6] and [38], where basic creep is creep without exchange of moisture with the environment whereas drying creep is taking place with exchange of moisture. However the separation is problematic because it is difficult to distinguish between self-dessication, [31], and exchange of moisture with the environment and therefore this separation is less suitable when formulating material models. The key point is that the activity of the moisture is changed.

Fig. 3.11 shows how moisture in principle is placed between two cement particles before initiation of hydration and the size of a cement particle is approximately $10\mu m$, [19].

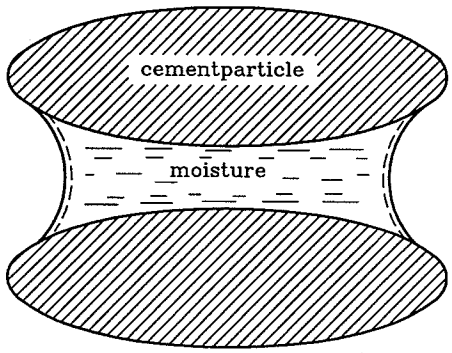

Figure 3.11: Principle structure of cement gel immediately after moisture addition.

For systems in thermodynamical equilibrium the curvature of the free water surfaces are given by the relative humidity in the adjoining areas through the Kelvin equation, [19] and [29]. Further in equilibrium the activity of the water in the cement gel is a function of

- temperature
- the relative humidity, pressure
- particle and moisture interaction, sorption phenomena

Increased temperature or increased relative humidity gives an increased activity of the water, [19], [4] and [5]. In the surface area between the moisture and the cement gel the

moisture is subjected to attractive forces from the cement gel and this reduces the activity of the water, [19], [1] and [46]. In [26] some experiments are made which show an influence from temperature gradients in time on the creep properties. It is observed that the creep increases significantly when the temperature vary.

Influence from stresses on the creep behaviour still need to be investigated, e.g. if there is a difference between creep in tension and compression. However, in [38] some experiments on creep in compression are mentioned where stresses at the early ages have reduced creep for sealed concrete. The influence from stresses on the strength development in time is documented, [38] and [17], where early stresses increases the strength.

The way stresses influence the mechanical behaviour at early ages is not clarified but it may be an effect similar to the temperature effect mentioned above where stresses influence the structure of the hydration products.

In experiments with hardened concrete, [45], it was found that the coefficient of thermal expansion is coupled to the relative humidity principally as shown in Fig. 3.12. It is likely that a similar phenomenon may be observed at early ages but at present little is known.

Figure 3.12: Dependence of the coefficient of thermal expansion on the relative humidity, [45].

Fig. 3.12 shows that the coefficient of thermal expansion for dry and old concrete and for saturated old concrete is smaller than for intermediate relative humidities. The specimens were tested in equilibrium at different relative humidities. In [17] experiments are reported where the coefficient of thermal expansion is different during heating than during cooling. The coefficient of thermal expansion has influence on the stresses generated from thermal gradients and a low value is preferable to avoid differential thermal cracking.

Another example on the couplings is the non-linear relationship between the diffusion coefficient and relative humidity, e.g. as shown in Fig. 3.13.

Fig. 3.13 shows that the diffusion coefficient, for relative humidities less than 0.6, is constant while it increases almost with a factor 20 in the range 0.6 to 0.8. The relationship shown in Fig. 3.13 is valid for hardened concrete but it seems reasonable to expect a similar behaviour for hardening concrete.

Time and loading are also coupled e.g. as found in [47] and shown in Fig. 3.14.

The concrete in Fig. 3.14 was loaded in compression after 56 days of hydration to the indicated constant stress-levels. The curves illustrate the development in time of the strains as a function of the stress level. For relative loadings above 0.7 the response is creep untill a failure limit whereas for loading below 0.7 the concrete creeps untill a creep limit. At the

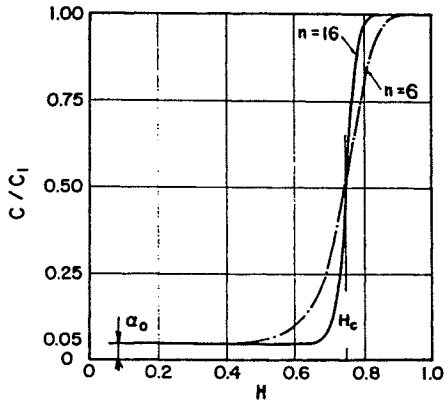

Figure 3.13: The dependence of the diffusion coefficient and the relative humidity, [7].

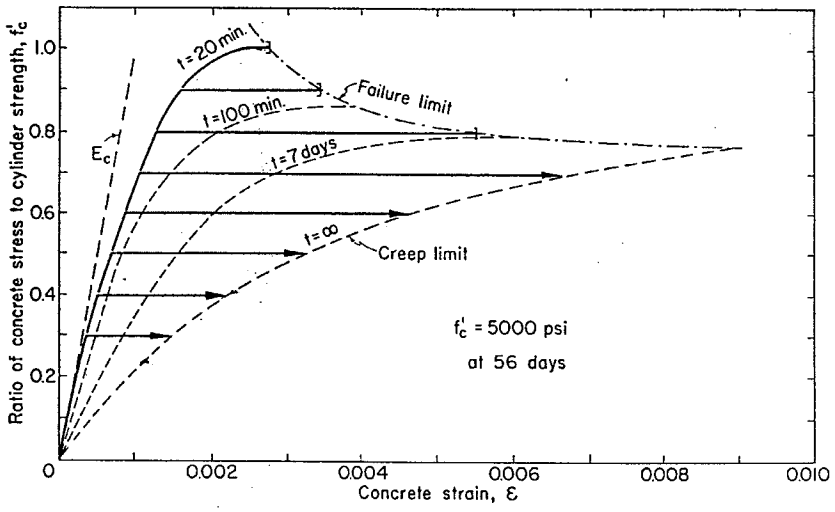

Figure 3.14: Development of strains as a function of the stress level, [47].

creep limit the load is carried without any further increase in deformations. For the high loadings the tensile strain capacity decrease with an increase in load. From experiments it is also known that a larger rate of loading gives a relative larger strength, but lower strain capacity, whereas slower loading rates decreases the strength, but increases the strain capacity. This sort of behaviour may be due to creep. For the larger loading rates creep does not have time to manifest.

The survey given above points out the factors, which give impact on the mechanical behavior of concrete at early ages. The factors should be brought in mind when the uncertainty of the modelling and the volume of the necessary experiments is discussed.

Chapter 4

Proposed Creep Model

It was shown in the previous chapter that creep

- influences the time dependent deformations
- influences the redistribution of stresses
- is influenced by temperature and moisture distributions

An incremental creep model based on a direct solution of the second order differential equation, for a Kelvin type rheologic model with age dependent moduli, is outlined. The model makes no separation between creep and relaxation, and thereby creep covers phenomena related to mechanical loading. The influence from temperature is included in the model using the activation energy principle and a model for the imbalance introduced as a result of changes in temperature and moisture distributions.

4.1 Rheologic Creep Model

The rheologic model in fig. 4.1 with one Kelvin cell is used as introductory example.

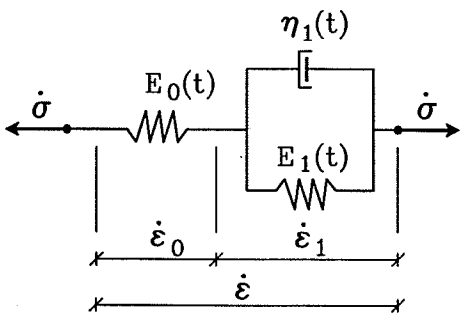

Figure 4.1: Rheologic model for the one-dimensional case.

The model in Fig. 4.1 consists of an initial spring, with stiffness $E_0(t)$ and a Kelvin cell, with a spring of stiffness $E_1(t)$ and a dashpot with the viscosity $\eta_1(t)$. The properties are

functions of time. The properties related to the springs are indexed with a superscript s and the properties related to the dashpots are indexed with a superscript d. Summing the strain increments in each element gives

$$\dot{\varepsilon} = \dot{\varepsilon}_0 + \dot{\varepsilon}_1 \tag{4.1}$$

The strain increment in the initial spring is

$$\dot{\varepsilon}_0 = \frac{\dot{\sigma}_0^s}{E_0(t)} \tag{4.2}$$

and this is the incremental equilibrium equation for a spring with an age dependent modulus of elasticity, [6], discussed before. The strain increment in the Kelvin cell is calculated from the incremental equilibrium equation

$$\dot{\sigma}_0^s = \dot{\sigma}_1^s + \dot{\sigma}_1^d \tag{4.3}$$

where $\dot{\sigma}_0^s$ is the total stress increment, $\dot{\sigma}_1^s$ is the stress increment in the spring and $\dot{\sigma}_1^d$ is the stress increment in the dashpot.
The stress increment in the spring, $\dot{\sigma}_1^s$, with stiffness E_1 is given as in (4.2)

$$\dot{\sigma}_1^s = E_1(t)\dot{\varepsilon}_1 \tag{4.4}$$

where $\dot{\varepsilon}_1$ is the strain increment in the Kelvin cell, as shown in fig. 4.1. The stresses in the dashpot, σ_1^d, is written

$$\sigma_1^d = \eta_1(t) \cdot \dot{\varepsilon}_1 \tag{4.5}$$

and differentiating this, taking into consideration the variation of the viscosity, $\eta_1(t)$, in time, the stress increment in the dashpot become

$$\dot{\sigma}_1^d = [\dot{\varepsilon}_1\dot{\eta}_1(t)] = \ddot{\varepsilon}_1\eta_1(t) + \dot{\varepsilon}_1\dot{\eta}_1 \tag{4.6}$$

Insertion of (4.4) and (4.6) in the equilibrium equation, (4.3), and rearranging gives

$$\ddot{\varepsilon}_1 + \frac{E_1(t) + \dot{\eta}_1(t)}{\eta_1(t)}\dot{\varepsilon}_1 = \frac{\dot{\sigma}_0^s}{\eta_1(t)} \tag{4.7}$$

which is the differential equation governing a Kelvin cell with time dependent properties. Solution of (4.7) is done in timesteps and the variation of the moduli are considered constants within each timestep, as shown in Fig. 4.2, with the modulus of elasticity as example.
A value corresponding to the center of the timestep is used for the entire timestep and thus inserting (4.4), for the incremental stress in the spring, into (4.7) and rearranging the second order differential equation becomes

$$\ddot{\varepsilon}_1 = \frac{1}{\eta_1(t)}(\dot{\sigma}_0^s - \dot{\sigma}_1^s) = \frac{\dot{\sigma}_1^d}{\eta_1(t)} \tag{4.8}$$

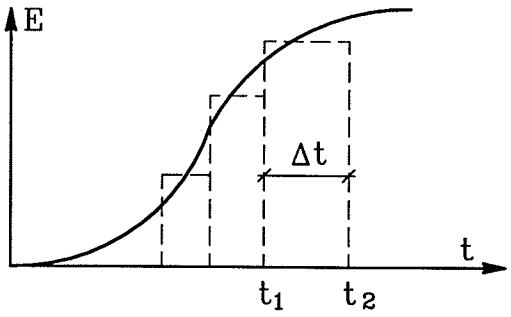

Figure 4.2: Discretisation of the modulus of elasticity.

and integration yields

$$\dot{\varepsilon}_1 = \frac{\sigma_1^d}{\eta_1(t)} \tag{4.9}$$

which gives the strain increment in the Kelvin cell. Using (4.1) and (4.2) the incremental constitutive equation becomes

$$\dot{\sigma}_0^s = E_0(t)(\dot{\varepsilon} - \dot{\varepsilon}_1) \tag{4.10}$$

and it is seen that the strains in the Kelvin cell may be interpretated as initial strains. The elastic modulus of the initial spring gives the short term deformations and the Kelvin cell gives the creep deformations.

The model shown in Fig. 4.1 may be extended with as many Kelvin cells as needed and in the present context we have chosen the arrangement in Fig. 4.3.

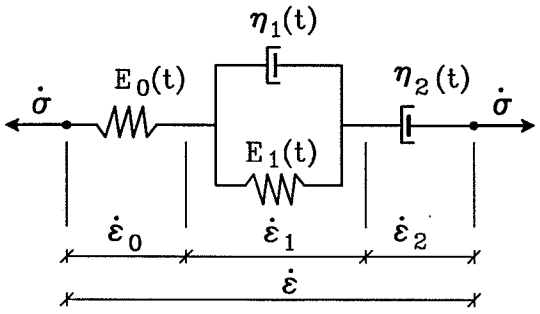

Figure 4.3: Rheologic model for the one-dimensional case.

A single dash-pot has been added and this is due to experimental observations showing that the creep when the concrete is loaded exceeds the creep following load removal i.e. η_2 represents this additional irreversible part of the total creep. Irreversibel creep deformations are also produced in the the Kelvin cell. One of the examples demonstrate this observation. The parameters in the model then consists of two elastic moduli, $E_0(t)$ and $E_1(t)$, and two viscosities, $\eta_1(t)$ and $\eta_2(t)$. The development in time of these properties is given by

- the hydration process
- the moisture distribution

The elastic moduli is assumed to depend on the skeleton of the concrete and the load carrying part of the water in the cement gel, [50] and [51]. Similarly is assumed for the viscosities, but in excess these properties are assumed to depend on the moisture redistribution. That is when water is moving the viscosity of the concrete is significantly influenced whereas the modulus of elasticity is not influenced. This separation is used when taking temperature effects into account. The load carrying capacity of the water in the cement gel is not assumed to depend on whether the water is being redistributed only on the actual level of the relative humidity.
The function chosen for the development of the modulus of elasticity in time is

$$E(t) = a \times exp(-(b/t)^c) \tag{4.11}$$

which is also used to describe several properties at early age in [15]. a, b and c are concrete dependent parameters which are determined from fitting of data. The development of the viscosity in time is given by

$$\eta(t) = a(1 - \exp(-bt))(1 - c\exp(-d|t - f|^e)) \tag{4.12}$$

where a, b, c, d, e and f are concrete dependent parameters. The first part of (4.12) is a general exponential development given by where a gives the final level and b gives the rate of growth. This general development is corrected to reflect the result of the preliminary data fitting that the viscosity increases only slightly initially and after about 200 hours the major increase takes place. The parameter c gives the magnitude of the correction, d and e the extension of the correction in time and finally f gives the location in time of the correction. Fig. 6.2 shows examples on the principle development given by the functions above. For the development of the properties in the case of a variable temperature history the maturity is used instead of time and the viscosity is further scaled, this is described later.

4.2 Temperature Effect

The influence of temperature on the development of the properties in the model is obtained from the activation energy principle. The activation energy is a measure of the energy needed to bring some chemical species in an activated state where a reaction is possible, [57]. The Arrhenius equation for a chemical process is the experimental observed fact, that the variation of the rate constant, k, with temperature is

$$k = A \times \exp(-\frac{U}{RT}) \tag{4.13}$$

where A is a constant, U is the activation energy, R is the gas constant and T is the absolute temperature. In our case several processes are active, e.g.

- reactions between water and cement
- diffusion of moisture

In the modelling we use one value of the activation energy to characterise the hydration process and one value to characterise the diffusion process and these values are denoted apparent activation energies.

For analysis of the influence from temperature on creep the parameters in the model are adjusted. The maturity concept is applied initially to correct the four parameters for the different rates of hydration. In this correction an activation energy of $U = 33.5$ kJ/mole is applied and this value has shown good agreement with experimental data on the compressive strength development, [20], when the temperature exceeds $20°C$. For lower temperatures the activation energy is temperature dependent.

The second value of the activation energy is used to model the influence from temperature on the diffusion process. Diffusion of moisture is assumed to increase with temperature because of the increased activity and the result of this is an increase in the rate of creep. Therefore the viscosities are reduced upon an increase in temperature with a temperature dependent factor. Since $\eta^{-1} \propto k$ this temperature dependency may be calculated using the Arrhenius equation. In [49] creep of hardened cement paste was investigated and a value of $U_{\text{diffusion}} = 15.9$ kJ/mole were found to characterise the influence of temperature on the rate of creep. If we use the viscosity of water at 20 and $40°C$ to calculate an activation energy we obtain $U_{\text{water}} = 16.4$ kJ/mole and this is very close to the one obtained in [49]. The reduction factor is calculated based on a reference temperature, chosen to $20°C$ in the examples. The development of the viscosity at the reference temperature is considered as a basis and for other temperatures this basis viscosity is reduced. The reduction factor is similar to the rate coefficient, H, used in the maturity principle, (3.2), only a value of the activation energy of $U_{\text{diffusion}}$ is used.

The incorporation of the temperature effect as described above include the influence from different constant temperature levels and to include also the effect from gradients an imbalance, S, is introduced. Fig. 4.4 shows a neck between two cement gel surfaces and the types of water which are

- vapor
- capillary water
- adsorbed water
- hindered adsorbed water

The cement gel is characterised by thin spaces where adsorbed moisture may not accomodate completely and from thermodynamic considerations, [4] and [5], it appear that large local stresses can exists in these environments. In Fig. 4.4 this correspond to the hindered adsorbed water and the stresses are termed the disjoining pressure. Further due to the presence of minisci the capillary water is subjected to underpressure termed capillary pressure. The disjoining pressure and the capillary pressure depend on both the changes of

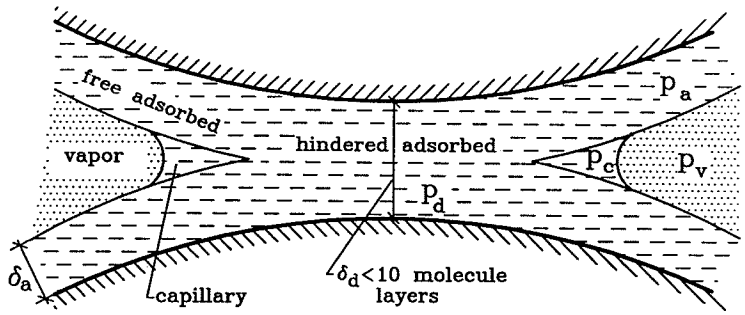

Figure 4.4: Types of water between two cement gel surfaces.

temperature and moisture distribution. In [9] it was shown how the influence from moisture on the local stresses could be used in a material model to model the Pickett effect. Here the imbalance, S, is used to measure the effect from the local stresses and include S as one of the memory variables in the model. The role of the imbalance S is then to remember the moisture and temperature history of the material, and in the present context we are only interested in temperature effects. Using the imbalance in the model is an attempt to relate the parameters in the model to the physical processes in the concrete.

We need an evolution law for the imbalance and the simplest possible one is chosen

$$\dot{S} + cS = a\left|\dot{T}\right| \tag{4.14}$$

where c and a are two new material parameters that have been introduced. To solve (4.14) we further need the initial value of the imbalance, S_0. It is seen that for a constant temperature the imbalance decreases in time exponentially and when temperature gradients are present the imbalance decreases slower or it may increase depending on the magnitude of the gradients. It is assumed that higher imbalance gives a more mobile structure of the cement gel and thus larger strain increments and therefore the strains produced due to the imbalance are written

$$\dot{\varepsilon}_S = kS\sigma \tag{4.15}$$

where σ is the stress and k is a material parameter. The relation given in (4.15) corresponds to a dash-pot with a viscosity given as

$$\eta_3 = \frac{1}{kS} \tag{4.16}$$

and then the elements of the model are the ones shown in Fig. 4.5. The parameters introduced in relation to the microprestress term are presently all constant in time. However one could imagine that some of them would depend on the progress of hydration, e.g. due to the increased internal surface where adsorption may take place.

The constitutive model obtained now are

$$\dot{\sigma}_0^s = E_0(t)(\dot{\varepsilon} - \dot{\varepsilon}_i) \tag{4.17}$$

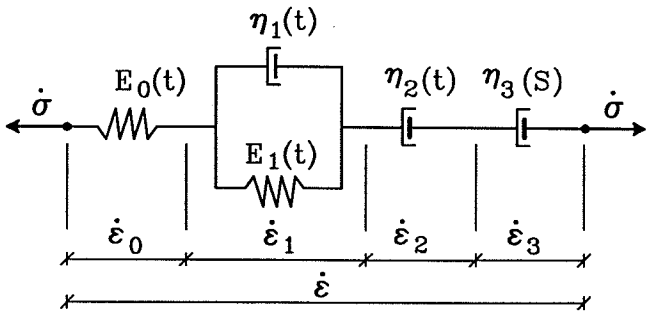

Figure 4.5: The elements of the material model.

where the initial strains are given by

$$\dot{\varepsilon}_i = \dot{\varepsilon}_1 + \dot{\varepsilon}_2 + \dot{\varepsilon}_3 \tag{4.18}$$

This concept of using the imbalance is open for inclusion of other effects e.g. the moisture distribution.

4.3 Generalisation to 3D

In the generalization to three dimensions the result from above is used and instead of scalar properties, matrices are used, and this is shown in fig. 4.6.

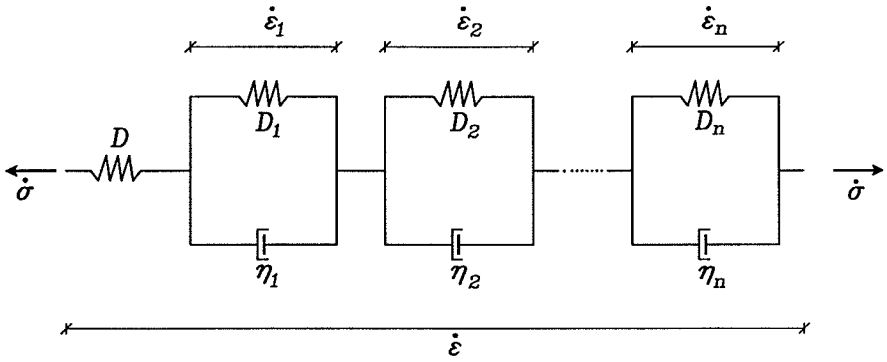

Figure 4.6: Generalisation of the material law to 3D.

Instead of one Kelvin cell the general formulation includes n cells coupled in series, and the following column matrices are introduced

$$\dot{\boldsymbol{\varepsilon}} = \left[\dot{\varepsilon}_x\, \dot{\varepsilon}_y\, \dot{\varepsilon}_z\, \dot{\phi}_{yz}\, \dot{\phi}_{xz}\, \dot{\phi}_{xy}\right]^T \tag{4.19}$$

for the incremental strains

$$\boldsymbol{\sigma} = \left[\sigma_x\, \sigma_y\, \sigma_z\, \tau_{yz}\, \tau_{xz}\, \tau_{xy}\right]^T, \qquad \dot{\boldsymbol{\sigma}} = \left[\dot{\sigma}_x\, \dot{\sigma}_y\, \dot{\sigma}_z\, \dot{\tau}_{yz}\, \dot{\tau}_{xz}\, \dot{\tau}_{xy}\right]^T \tag{4.20}$$

for the stresses and incremental stresses respectively

$$\dot{\boldsymbol{\varepsilon}}_{\boldsymbol{j}} = \left[\dot{\varepsilon}_x^j \dot{\varepsilon}_y^j \dot{\varepsilon}_z^j \dot{\phi}_{yz}^j \dot{\phi}_{xz}^j \dot{\phi}_{xy}^j\right]^T \tag{4.21}$$

for the initial strains in Kelvin cell number j and finally the stresses in the spring and dashpot of the $j'th$ Kelvin cell, $\boldsymbol{\sigma}_j^s$ and $\boldsymbol{\sigma}_j^d$ respectively

$$\boldsymbol{\sigma}_{\boldsymbol{j}}^{\boldsymbol{s}} = \left[\sigma_x^{js} \sigma_y^{js} \sigma_z^{js} \tau_{yz}^{js} \tau_{xz}^{js} \tau_{xy}^{js}\right]^T \tag{4.22}$$

and

$$\boldsymbol{\sigma}_{\boldsymbol{j}}^{\boldsymbol{d}} = \left[\sigma_x^{jd} \sigma_y^{jd} \sigma_z^{jd} \tau_{yz}^{jd} \tau_{xz}^{jd} \tau_{xy}^{jd}\right]^T \tag{4.23}$$

In practical computation the stresses in the springs of the Kelvin cells, $\boldsymbol{\sigma}_j^s$, are not stored since they may be obtained from equilibrium. The stresses in the dashpots, $\boldsymbol{\sigma}_j^d$, however are stored as internal stresses, a memory-variable, because they are used to calculate the strain increments in

$$\dot{\boldsymbol{\varepsilon}}_j = \boldsymbol{\eta}_j^{-1} \boldsymbol{\sigma}_j^d \tag{4.24}$$

where $\boldsymbol{\eta}_j$ is a matrix containing the viscosities related to the dashpot in the $j'th$ Kelvin cell. This is equivalent to using a matrix instead of the scalar compliance function. The internal stresses are the driving force in the basic mechanism of moving the stresses from the dashpots to the spring in the Kelvin cells.

The initial strains in the Kelvin cells are found by summation over the n cells

$$\dot{\boldsymbol{\varepsilon}}_i = \Sigma_{j=1}^n \dot{\boldsymbol{\varepsilon}}_j = \Sigma_{j=1}^n \boldsymbol{\eta}_j^{-1} \boldsymbol{\sigma}_j^d \tag{4.25}$$

The internal stresses, $\boldsymbol{\sigma}_j^d$, at the end of the timestep are not known in advance and thus iterations are needed. The stress increments in each Kelvin cell are equal.

$$\begin{aligned} \dot{\boldsymbol{\sigma}} = \boldsymbol{D}\dot{\boldsymbol{\varepsilon}}_0^s &= \dot{\boldsymbol{\sigma}}_1^s + \dot{\boldsymbol{\sigma}}_1^d = \cdots \\ &= \dot{\boldsymbol{\sigma}}_j^s + \dot{\boldsymbol{\sigma}}_j^d = \cdots = \dot{\boldsymbol{\sigma}}_n^s + \dot{\boldsymbol{\sigma}}_n^d \end{aligned} \tag{4.26}$$

and the stress increment in the $j'th$ spring is given as

$$\dot{\boldsymbol{\sigma}}_j^s = \boldsymbol{D}_j \dot{\boldsymbol{\varepsilon}}_j \tag{4.27}$$

The general form of the imbalance strain increments given by (4.15) is written

$$\dot{\boldsymbol{\varepsilon}}_3 = kS\boldsymbol{\sigma} \tag{4.28}$$

where it is assumed that the effect of the imbalance is isotropic since it only depends on the moisture and temperature history. The total model for 3D is the one shown in 4.5 and thus imbalance term is the third element. The strains given in (4.28) should be added to the initial strains from the Kelvin cells, (4.25) to have the total time-dependent strains.

Using (4.21) - (4.23) the incremental constitutive creep formulation for a general three-dimensional case is

$$\dot{\boldsymbol{\sigma}} = \boldsymbol{D}(\dot{\boldsymbol{\varepsilon}} - \dot{\boldsymbol{\varepsilon}}_i) \tag{4.29}$$

and this form is suited for analysis with finite elements.

Chapter 5

Implementation of Material Model

The numerical method aimed at here for solution of the coupled problems at early age is the finite element method. The effects of interest in the numerical analysis are the development of the moisture field, temperature field and the stresses as shown in Fig. 5.1 together with their mutual dependencies.

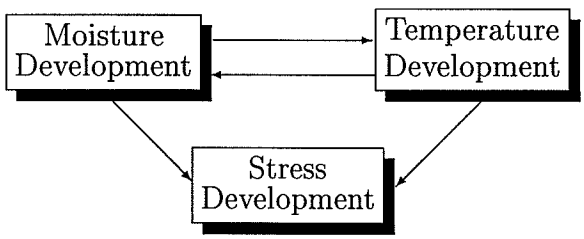

Figure 5.1: Couplings of the effects in the solution.

The dependencies are one-way from the moisture- and temperature development to the stress development whereas the relation between moisture and temperature is two-way. When the moisture- and temperature fields are changing during hydration strains are produced and this gives stress changes. On the other hand these stress changes has no influence on the moisture- and temperature fields. The magnitude of the stress changes depend on the stiffness of the structure which is a function of the degree of hydration. An example on the two-way coupling between moisture and temperature is the transport properties. When the moisture content decreases due to hydration the heat diffusion coefficient also decreases and this has effect on the moisture diffusion coefficient. Due to this character of the dependencies the temperature and moisture fields may be calculated without consideration of the stresses but the mutual coupling need to be considered. Generally the development of the moisture- and temperature fields in time is slow but the changes in stress may be abrupt e.g. in relation to cracking.

5.1 Incremental Scheme

The principle of the numerical method is shown in Fig. 5.2 for a one-dimensional structure. The structure is completely fixed in the ends and emphasis is on the variation of stresses and temperature in time. For clarity the load consists of temperature load from the hydration process only.

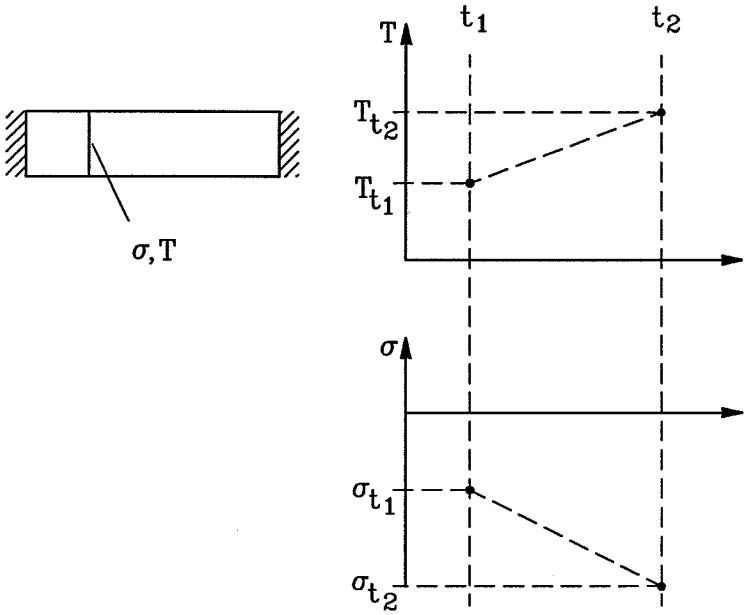

Figure 5.2: Projection of stresses and temperature respectively.

The solution procedure steps forward using finite timesteps, $\Delta t = t_2 - t_1$, from a known state characterised by the stress, σ_{t_1}, and the temperature, T_{t_1}. The problem is to find the state at time t_2 and incorporate the development of the material properties. Since this development depend on among other the temperature development which is unknown from t_1 to t_2 the solution procedure becomes non-linear. An iterative scheme is applied where linear projections of the stress and temperature as shown is made. Following this procedure of stepping forward in time is termed an incremental solution procedure.

Having established the new state at time t_2 a new timestep is applied where the starting point is the state just determined. In this way discrete states are calculated fulfilling the true development of the material properties and equilibrium.

5.2 Survey of the Solution Procedure

Fig. 5.3 gives a survey of the inclusion of the couplings in a numerical analysis. The loading may be due to mechanical, temperature, moisture and/or creep action, and creep only takes place in connection with another loading type. The last three loading types gives initial strains which are converted to equivalent mechanical load during the analysis.

An analysis of the involved effects are made where emphasised and the changes in the *Temperature* and the *Moisture* distribution are coupled to the mechanical problem through the

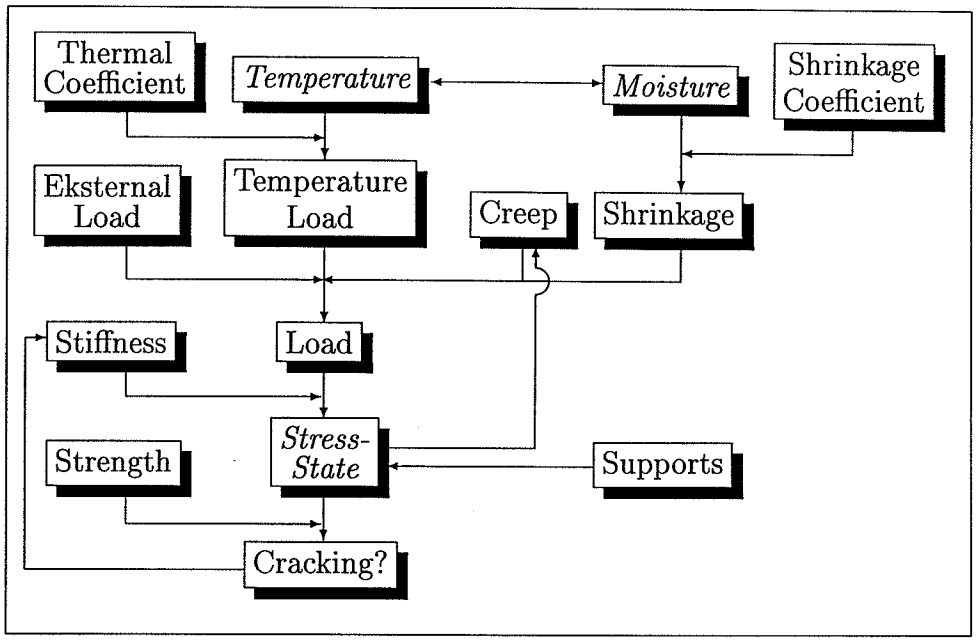

Figure 5.3: Consideration of couplings in numerical analysis.

coefficient of thermal expansion and the shrinkage coefficient. The progress of the hydration including the couplings as shown in Fig. 3.2 gives the development of the properties. The stress state depends on the supports, the equivalent load and the stiffness. Further the stresses gives feedback on the creep and in the case of cracking the stiffness is reduced.

Chapter 6

Analysis of VD Concrete

The proposed creep model is used for the analysis of the results from phase 1, 3 and 5 in the HETEK project which deals with the VD concrete. The examples cover creep at variable load history, creep in tension and compressive creep measured at different temperature histories. The material parameters obtained from the analysis of the compressive creep and creep at a variable temperature history are used to analyse the experimental results from a fixed specimen subjected to a prescribed temperature history. The stresses from the experiment are compared with numerical results and an acceptable accuracy is obtained.

6.1 DTI Measurements from Phase 1

In phase 1, [52], the concrete has been analysed using the test program presently in use at DTI. The concrete was mixed and delivered by 4K-Concrete in Copenhagen. Three loaded and three unloaded specimens are used in the creep test. The specimens are cast in an upright position in closed plastic forms. After casting insulation is made and the temperature is controlled with air. Steel inserts for the strain measuring devices are cast into the concrete and fixed to the forms. At setting time the forms are released but kept on the specimen to seal the concrete. By measuring the strains on all specimens and keeping the temperature constant it is possible to separate the strains due to mechanical load from the thermal and shrinkage strains.

The concrete is loaded in compression and the load history is chosen to provide information about the parameters used in the model. The age at loading for the first and second specimens were 14 hours and for the third specimen 30 hours. The temperature was kept constant at about $22°C$ except for a short peak up till $27°C$ at 12 hours. This peak has been taken into consideration in the modelling. Information about the complete experimental analysis of the concrete is given in [52] and [54] describes the test method.

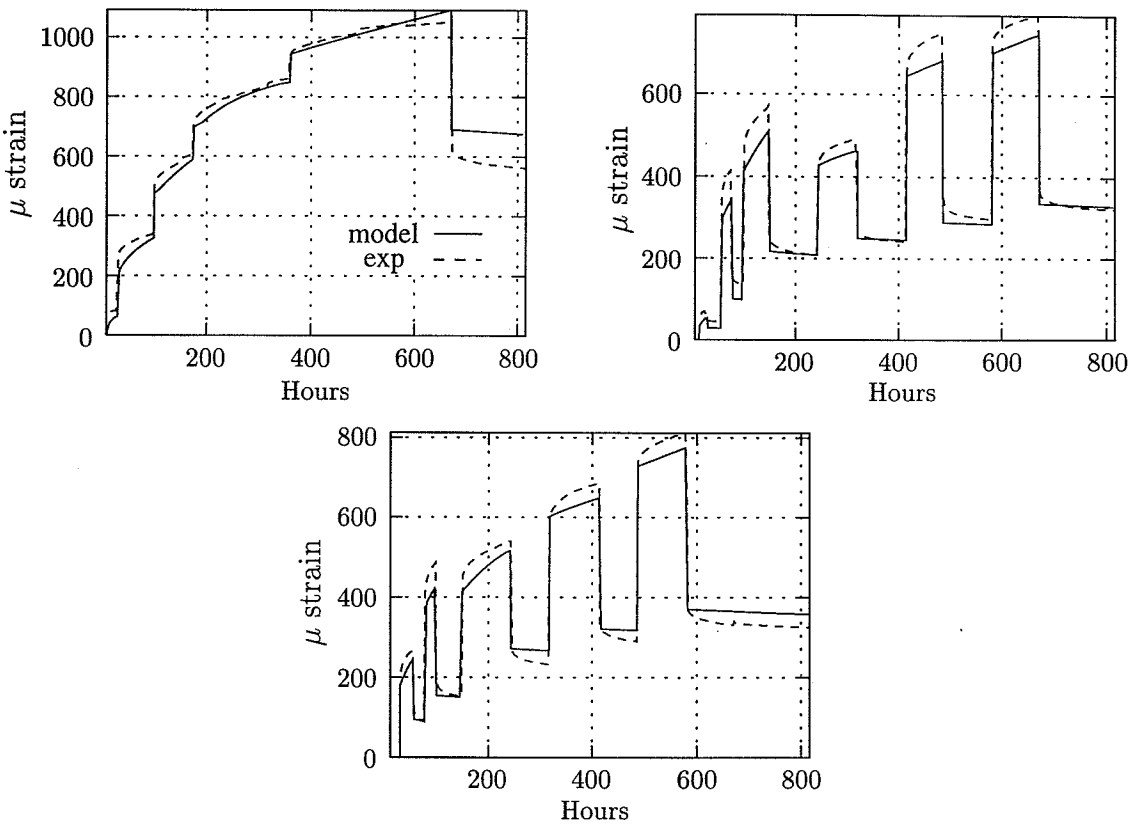

Figure 6.1: Fit of the results from phase 1.

Fig. 6.1 shows the measured creep due to mechanical loading for the three specimens. Also shown are the results obtained with the proposed model and a close fit is seen. The scatter between the numerical model and the experimental results is mainly due to the elastic part of the deformations. In the present fitting procedure both the elastic and the time dependent deformations are treated simultaneously. Another strategy, used by DTI [52], separates the elastic and the time dependent deformations. For the elastic part DTI either propose a Danish standard for the development of the modulus of elasticity or application of the information about the moduli of elasticity obtained from the creep measurements. The two strategies gives different results. In the present method the deviations on the total deformations are minimized, whereas DTI minimizes the deviations on the time dependent deformations. The deviations on the elastic deformations do not appear directly in the DTI fit of the creep part, as the values measured in the tests are used.

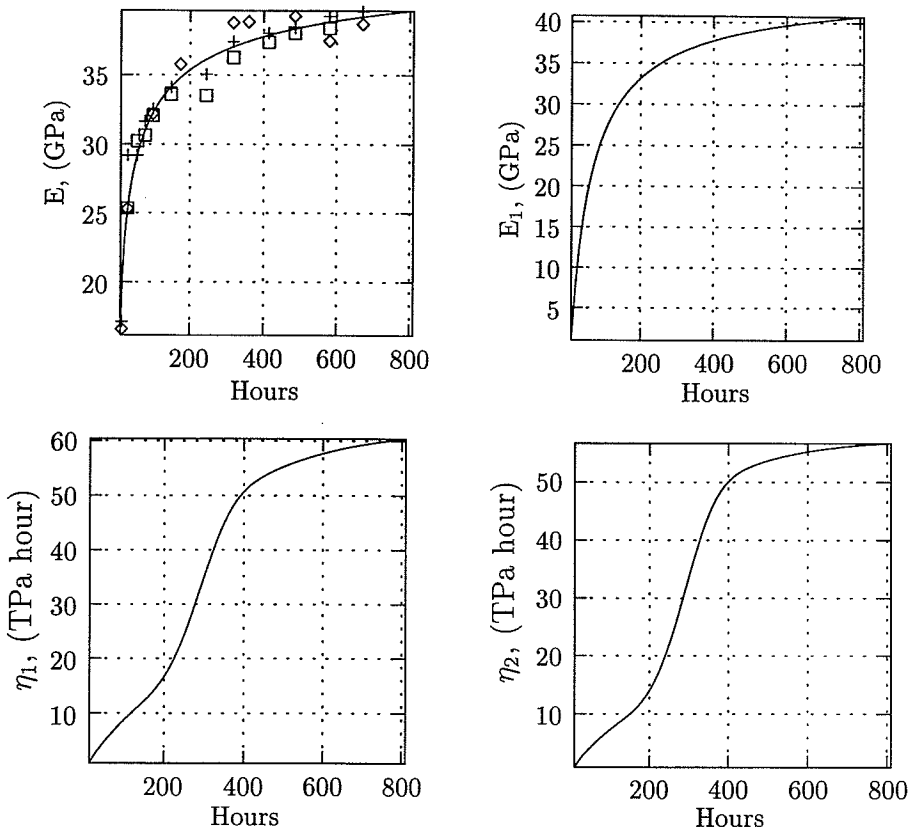

Figure 6.2: Parameters used to fit phase 1 results.

The optimal development of the moduli of elasticity are given by (4.11) and the parameters shown in Table 6.1.

	a (MPa)	b (hour)	c
E	45.0 10^3	10.0	0.46
E_1	45.0 10^3	50.0	0.8

Table 6.1: Optimal development of the moduli of elasticity.

The optimal development of the reference viscosities are given by (4.12) and the parameters shown in Table 6.2.

	a (TPa hour)	b (hour^{-1})	c	d (hour^{-1})	e	f (hour)
η_1	65.0	0.004	0.6	5.0 10^{-9}	3.5	100.0
η_2	60.0	0.005	0.7	5.0 10^{-9}	3.5	100.0

Table 6.2: Optimal development of the viscosities.

The parameters are shown in Fig. 6.2 and they are two elastic moduli and two viscosities. The measured elastic moduli are shown to be close to the curve used for fitting the

properties in the instantaneous spring.

6.2 DTU Measurements

The measurements of creep in tension reported in [26] have been analysed with the proposed model. Since the mix-proportion is identical with the one used for the compressive results shown in Fig. 6.1 the tensile creep results are analysed with the same parameter set as shown in Fig. 6.2. The parameter values for the material properties used are shown in Table 6.1 and Table 6.2.

6.2.1 Tensile Creep, Phase 3

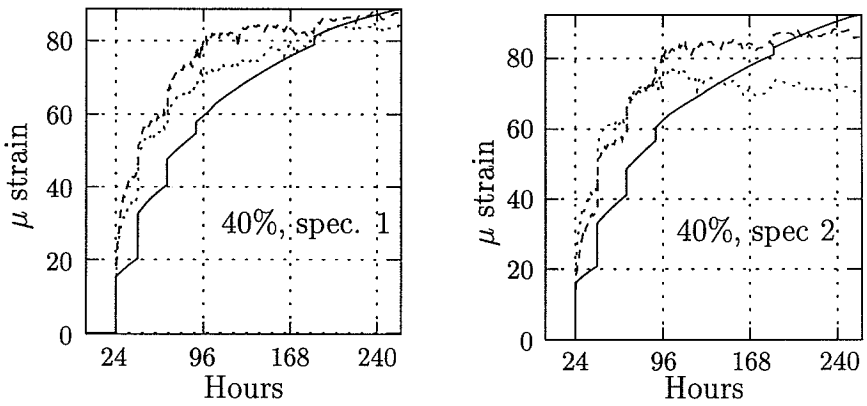

Figure 6.3: Tensile creep, 24 hours and 40% load.

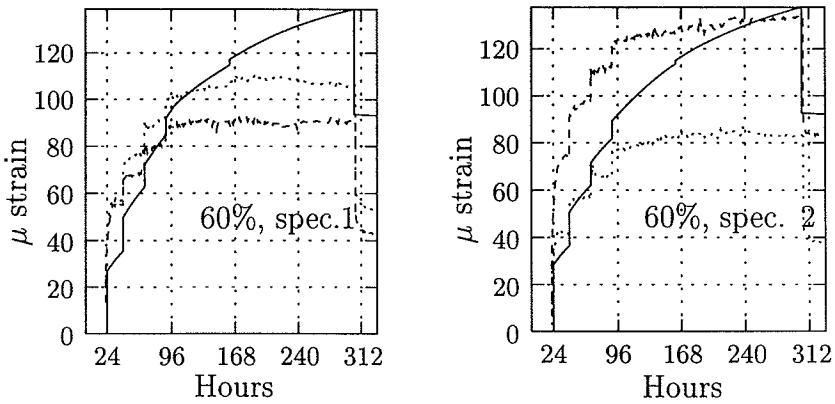

Figure 6.4: Tensile creep, 24 hours and 60% load.

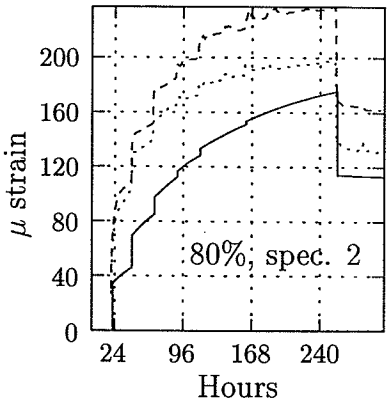

Figure 6.5: Tensile creep, 24 hours and 80% load.

Fig. 6.3 to 6.5 shows the measured tensile creep for the concrete loaded after one day of hardening at about $20°C$ together with the numerical results. For each specimen the measured result on both sides of the specimens are shown and this is because some skewness was observed in the tests. Only one specimen is shown for the stress level of 80% and this is because the other failed shortly after loading. The failure load was found to be 2.85 MPa which is close to the tensile strength measured on the dogbone specimens, [26]. At the load level 40% the tendency is that the numerical results are close to the measured creep whereas the conclusion is more uncertain in the case of the 60% load level. At 60% load level is seems like the deformations stop and this may be due to the sensitivity of the LVDT's. However, for the highest load level, 80% and loaded after 24 hours, the result is clear and it shows that the numerical result underestimate the measured creep. This indicate that some non-linearities are present and to quantify this more experiments are needed. From Fig. 6.3 to 6.5 it seems like creep in tension at the two lowest load levels stop after some time whereas the deformations continue to grow at the highest load levels.

A similar analysis was carried out for the concrete loaded after 72 hours of hardening and Fig. 6.6 to 6.7 shows the result. Due to the skewness indicated the conclusions are uncertain. However, it may be that the measurements on one side stopped while the other continued and this gives acceptable results.

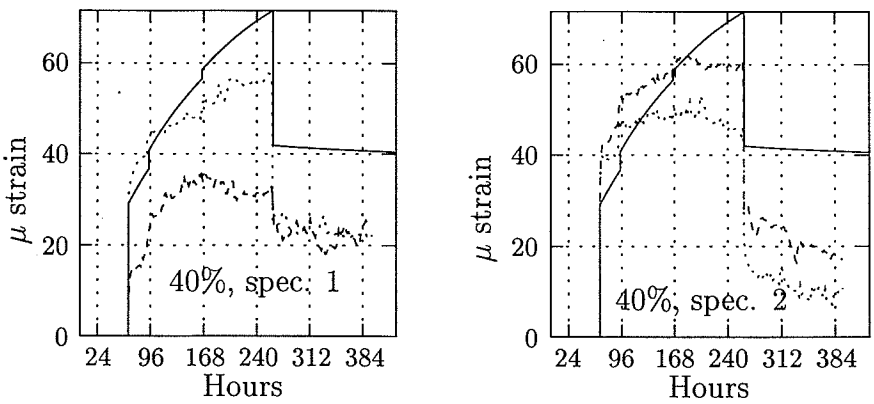

Figure 6.6: Tensile creep, 72 hours and 40% load.

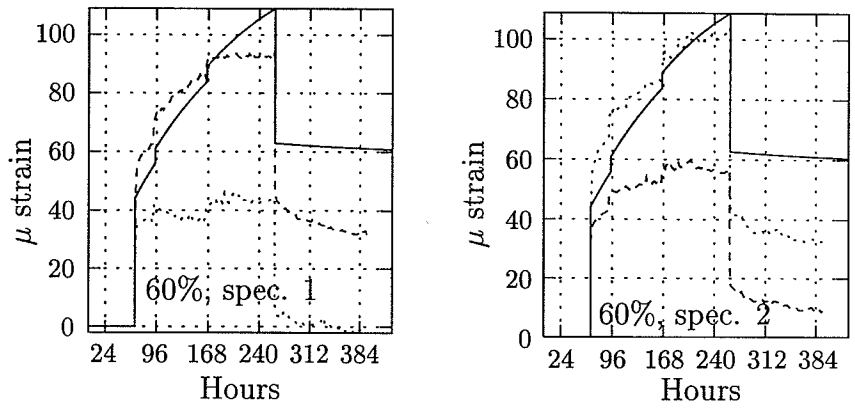

Figure 6.7: Tensile creep, 72 hours and 60% load.

Generally it seems like creep in tension is of the same order of magnitude as creep in compression. However, at higher load levels some non-linearities was observed.

6.2.2 Compressive Loading and Temperature, Phase 3

The temperature histories used in the numerical analysis are shown in Fig. 6.8 and they correspond to the measured temperatures, reported in [26].

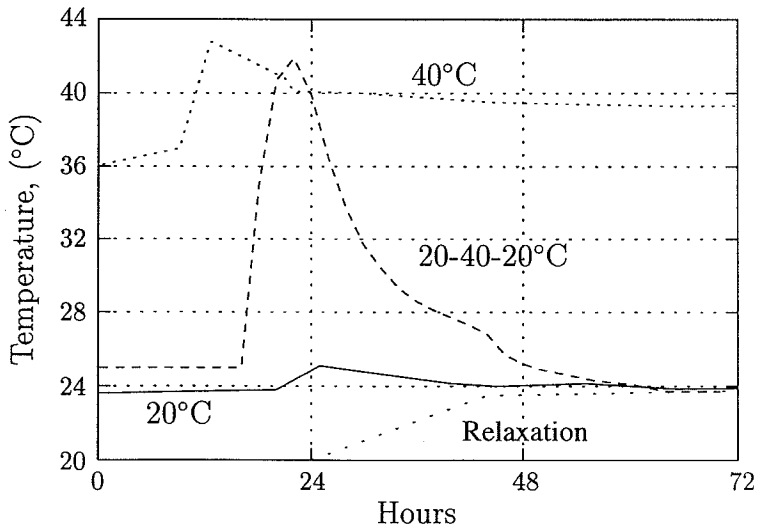

Figure 6.8: Temperature history.

The compressive creep measurements at 20 and $40°C$, respectively, are shown in Fig. 6.9 together with the numerical results. The numerical results are obtained using the parameters in Fig. 6.2. The agreement seems to be acceptable when comparing with an enlarged part of the compressive creep shown in Fig. 6.10. For the $40°C$ test Fig. 6.9 shows the numerical results both with and without the reduction of the viscosities due to diffusion. The slope of the numerical curve without the correction is smaller than with the correction because the viscosities are larger.

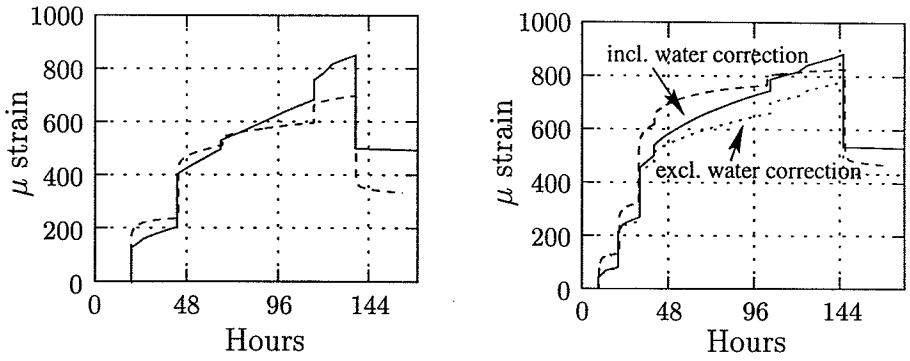

Figure 6.9: Creep measured and fitted at 20 and 40°C.

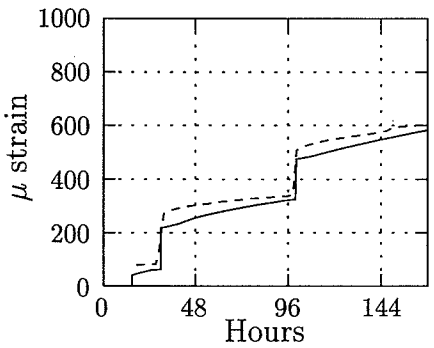

Figure 6.10: Enlarged part of fit from phase 1.

Fig. 6.11 shows the numerical results for the variable temperature history and some discrepancies are observed. However, as shown the contribution from the microprestresses significantly improves the numerical results. If the microprestress term was left out of the analysis only about 30% of the ultimate measured creep would be predicted. The numerical result including the microprestress term seems to be lower than the measured result particularly in the first hours after application of load. In the analysis an average temperature was used because the temperature measurement taken in one point was used as representative for the complete specimen. Then the development in time of the spatial gradients in temperature are ignored. Following this average procedure the influence from gradients in time of the temperature are reduced and this may explain some of the difference. In a full 3D analysis of the specimen the development of the temperature profiles in time should be included. In [9] this was done for the influence of the development of the moisture distribution in time. Some of the difference may also be explained by the simple evolution law for the microprestresses where the material parameters in the present context are assumed to be independent of the hydration process. However, little is known about the processes of water diffusion in the microstructure and the influence on the microprestresses at present. To formulate a detailed model more information about these subjects are needed.

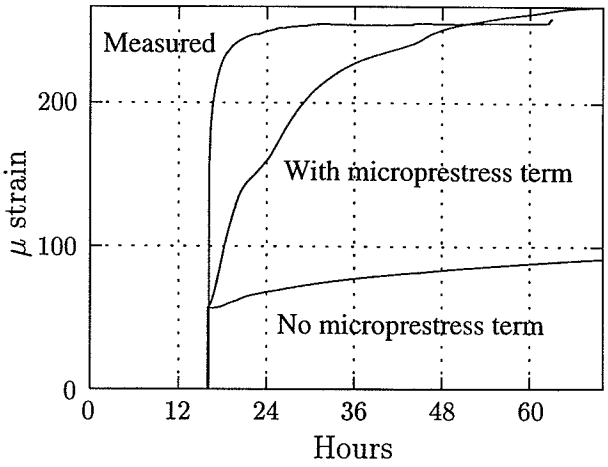

Figure 6.11: Creep measured and fitted at 20-40-20°C.

Fig. 6.12 shows the result of the analysis of the relaxation experiment and the agreement is acceptable. The development of the microprestresses at the different temperature histories are shown in Fig. 6.13 and it is seen that when the temperature changes the microprestresses increases. The optimal parameters governing the microprestress term are shown in Table 6.3.

S_0 (MPa)	c (hour^{-1})	a (MPa/°C)	k ((MPa)$^{-1}$/hour)
25.0	1.5	3.0	2.0 10^{-6}

Table 6.3: Optimal parameters for the microprestress term.

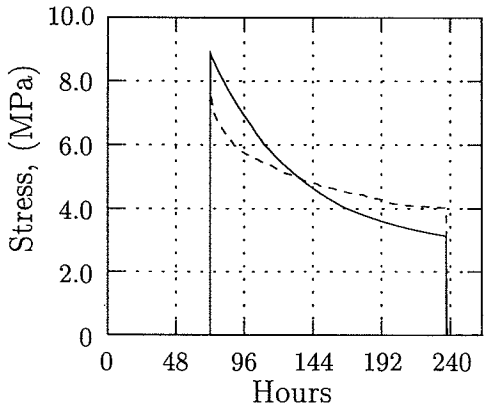

Figure 6.12: Relaxation fitted and measured at 20°C.

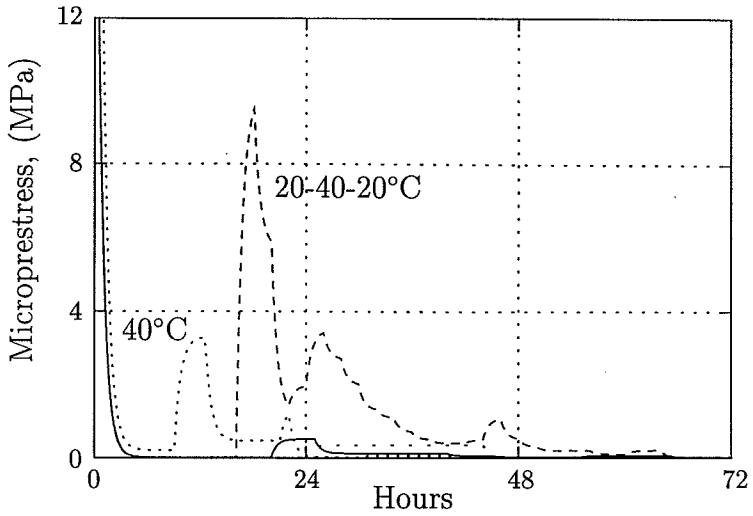

Figure 6.13: Development of microprestress.

The development of the properties in the springs and dashpots are shown in Fig. 6.14 and 6.15 The basis development at $20°C$ are identical to the parameters shown in Fig. 6.2. The differences seen are due to the correction in accordance with the temperature histories. Fig. 6.14 shows the development after the maturity correction and Fig. 6.15 shows the development of the viscosities after the diffusion correction.

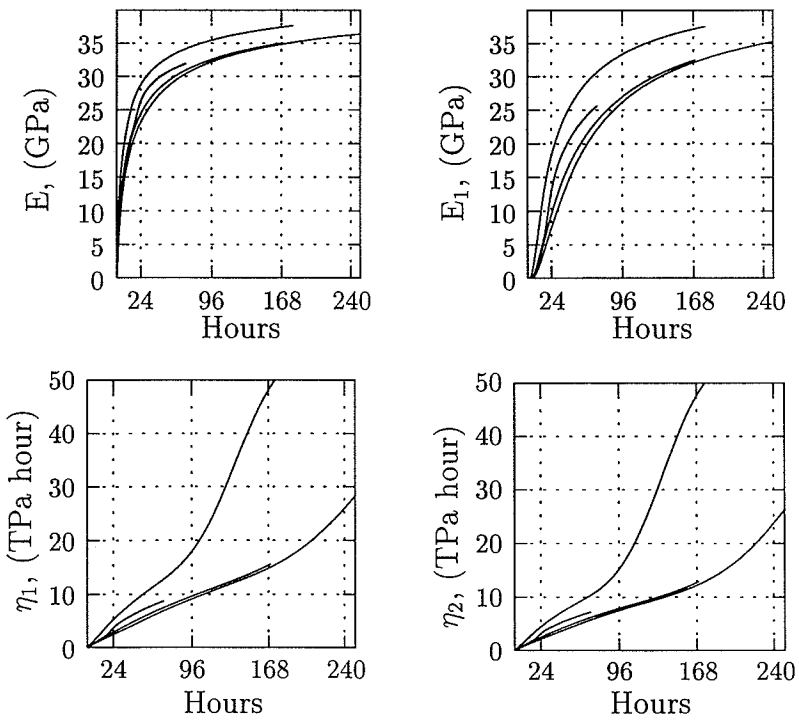

Figure 6.14: Material properties after maturity correction.

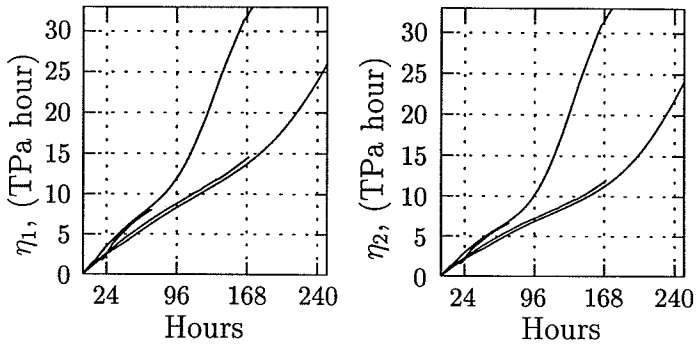

Figure 6.15: Viscosities after diffusion correction.

6.2.3 Discussion of DTU Measurements

The results of the numerical analysis of the tensile creep and compressive creep at different temperature histories indicated that the proposed model was able to include some of the couplings with a sufficient accuracy. In the analysis one set of material parameters was used and this is a restriction which need to be taken into consideration when evaluating the results. The individual results could be improved e.g. if the moduli of elasticity measured in the experiments when changing the load levels were used or several set of parameters were used. However, the idea was to see what could be done with one model and the obtained results are acceptable.

Another issue which need to be considered is the variation in the concrete from batch to batch which may be quite large. In our case the measured air content immediately after mixing was in the range from 3% to 5%. From previous experience it is known the a change in air content with 1% changes the material properties with 5-10%. Further adsorbed water in the aggregate may influence the properties. When making experiments there are also a general uncertainty and in the present context this influenced the results because the measurements of temperature influence and creep in tension are non-trivial.

6.2.4 Documentation of model with VD-concrete, Phase 5

Having obtained the material parameters for the VD concrete as described above an experiment is carried out where a one-dimensional specimen is subjected to a prescribed strain history as shown in Fig. 6.16. The purpose is to verify that sufficient information about the concrete is obtained and that the stresses may be calculated with sufficient accuracy. Chosing a one-dimensional specimen eliminates interactions between different parts of the structure and makes the restraints well-defined. Two axi-symmetric specimens were cast and stored in the temperature controlled shed as described in [26]. One of the specimens is an unloaded dummy and the other one is kept as fixed as possible in the developed frame. Fig. 6.16 shows the obtained strain histories in the two specimens. Each curve is the average of measurements from the two sides of the specimen and some skewness was observed. However, the average curves looks acceptable considering the accuracy observed in the measurements reported in [26]. The strains measured on the dummy represent both

shrinkage and thermal deformations. The maximum strains measured on the fixed specimen are smaller than that measured on the dummy specimen. The difference between the two curves is used as load in the numerical analysis and model the influence of the fixed supports. A step is observed on the fixed curve and this is due to a displacement of the piston in the frame.

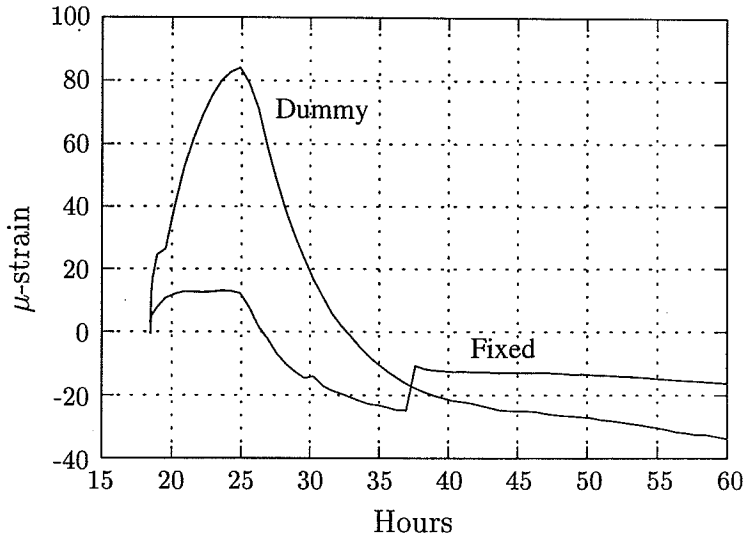

Figure 6.16: Loading on fixed specimen.

The temperatures of the specimens are controlled to model a situation likely to occur in practice and Fig. 6.17 shows the obtained temperature history in the fixed specimen. This temperature development is used as input in the material model to correct the material parameters.

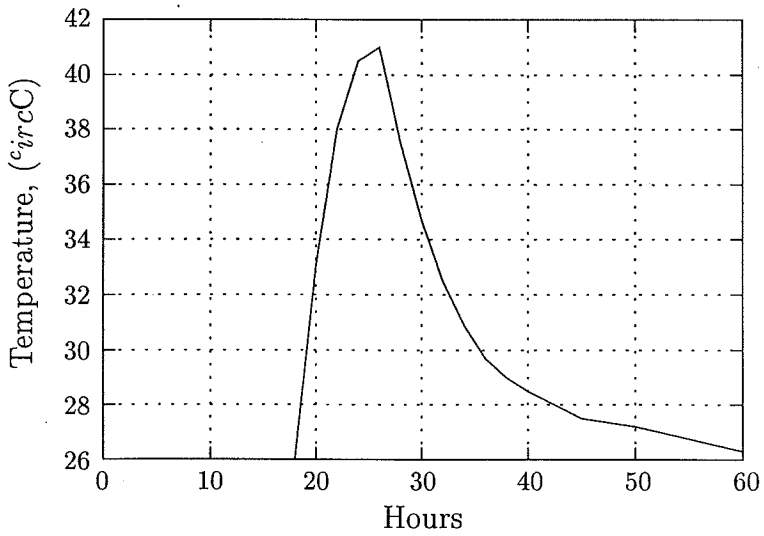

Figure 6.17: Temperature history.

Fig. 6.18 shows a comparison between the measured and calculated stress histories in the fixed specimen. The specimen was fixed after 15 hours of hydration and in the first 15 hours

compressive stresses developed due to the thermal expansion which offsets the shrinkage in this period. This heating was both due to the hydration and the artificial heating of the shed. The compressive stresses reaches their maximum after 25 hours of hydration. Subsequently tensile stresses are build up due thermal contraction and shrinkage.

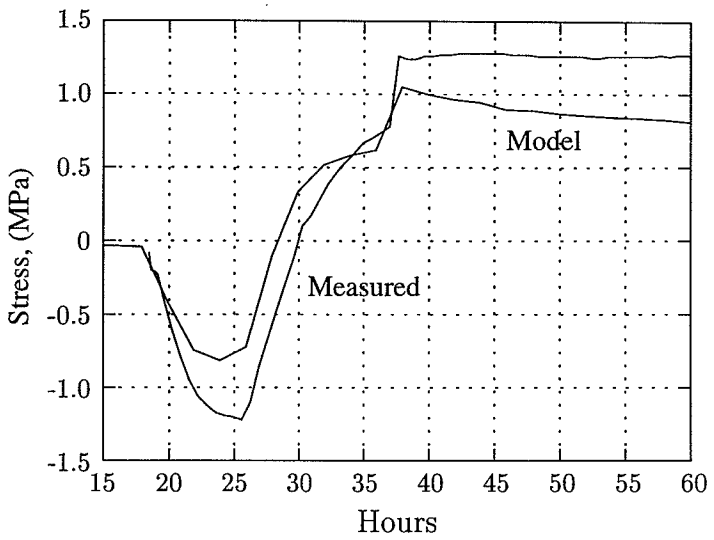

Figure 6.18: Experimental and numerical results.

The step of the piston caused the stress step also observed on the measured stress curve. This does not disturb the analysis because the stress step is equal to the strain step times the modulus of elasticity at the actual time. Both the compressive and tensile stresses obtained in the numerical analysis are underestimated with 30%. This is an acceptable accuracy because of the scatter observed in the experiments.

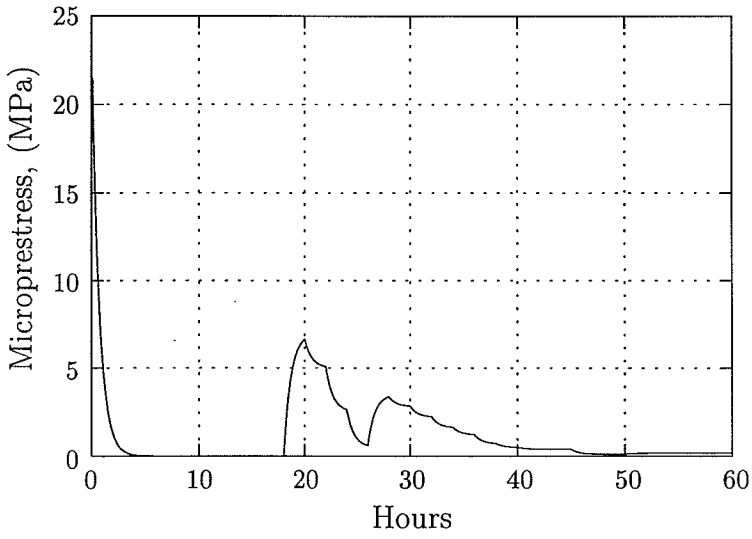

Figure 6.19: Development of microprestresses.

Fig. 6.19 shows the development of the microprestresses as a result of the temperature history shown in Fig. 6.17. Based on the present analysis it is concluded that the material

parameters obtained from the compressive DTI creep measurements and the compressive creep measurements at a variable temperature history provide sufficient information for a stress analysis.

Chapter 7

Alternative Concrete, Phase 6

After the analysis of the VD concrete an improved test program may be summarised

- compressive creep measurements, as the current DTI practice
- compressive creep at a variable temperature history

The purpose of the present analysis is to repeat the test program for an alternative concrete, described in [53], and obtain the material parameters. The material parameters are used for an analysis of a one-dimensional test specimen subjected to a prescribed strain history. The temperature history correspond to a situation from practice. This experiment is similar to the documentation experiment carried out for the VD concrete.

7.1 DTI Measurements, Phase 6

In phase 6, [53], the alternative concrete has been analysed using the test program presently in use at DTI. The concrete was mixed and delivered by Unicon I/S, Hedehusene.

Fig. 7.1 shows the measured creep due to mechanical loading for the three specimens. Also shown are the results obtained with the proposed model and a close fit is seen. The scatter between the numerical model and the experimental results is mainly due to the elastic part of the deformations. In the present fitting procedure both the elastic and the time dependent deformations are treated simultaneously. Another strategy, used by DTI [52], separates the elastic and the time dependent deformations. For the elastic part DTI either propose a Danish standard for the development of the modulus of elasticity or application of the information about the moduli of elasticity obtained from the creep measurements. The two strategies gives different results. In the present method the deviations on the total deformations are minimized, whereas DTI minimizes the deviations on the time dependent deformations. The deviations on the elastic deformations do not appear directly in the DTI fit of the creep part, as the values measured in the tests are used.

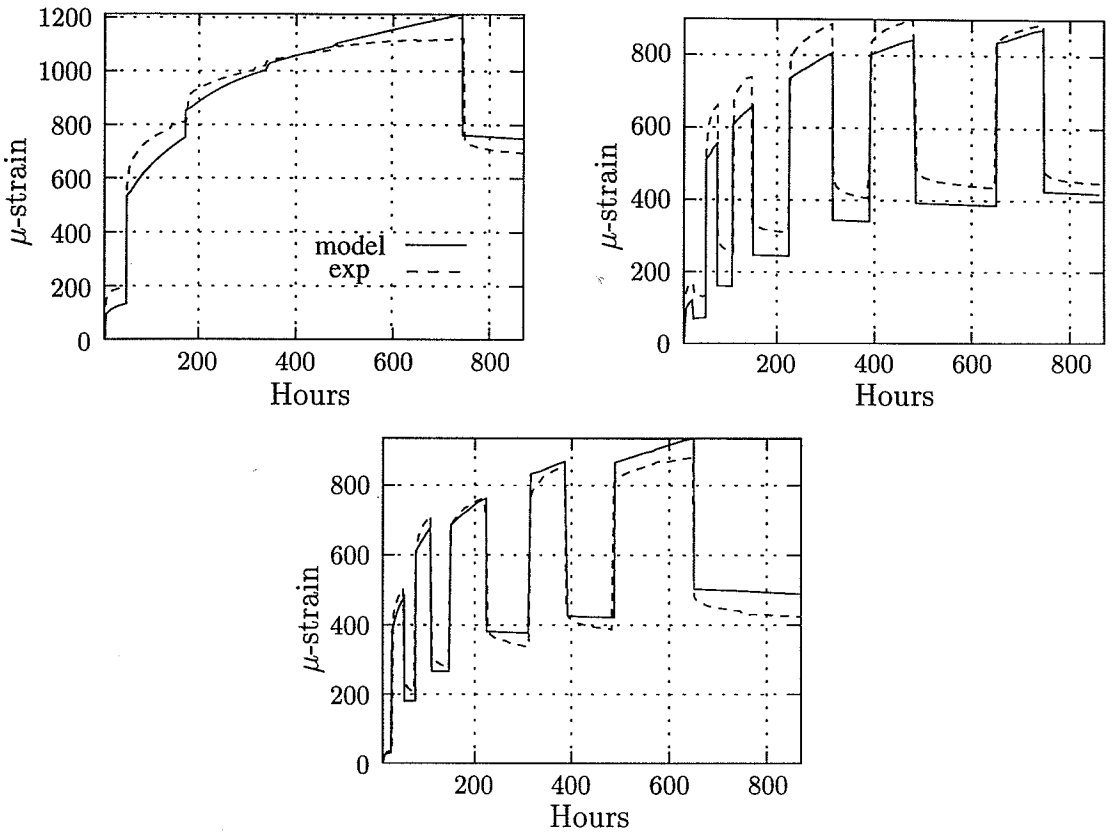

Figure 7.1: Fit of the results from phase 6.

7.2 DTU Measurements, Phase 6

The temperature development of the specimens used in Fig. 7.1 are almost constant except a short peak to $27°C$ after 18 hours of hydration. These temperature variations are taken into consideration in the analysis and used together with the compressive creep measured at a variable temperature history, shown in Fig. 7.2, for calibration of the thermal parameters.

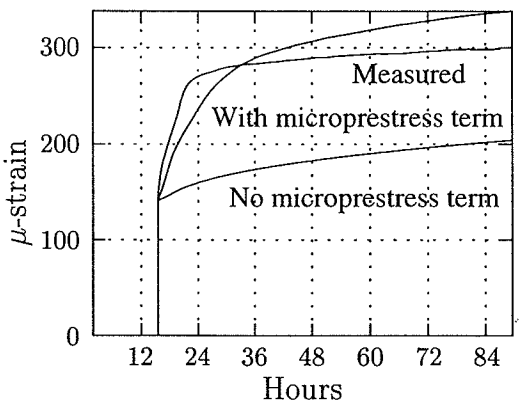

Figure 7.2: Fit of creep at 20-40-20$°C$.

The measured results shown in Fig. 7.2 are obtained following a procedure similar to the one reported in [26]. The numerical results are shown both when including the microprestress term and leaving it out. It is seen that including the microprestress term significantly improves the results. The optimal development of the moduli of elasticity are given by (4.11) and the parameters shown in Table 7.1.

	a (MPa)	b (hour)	c
E	40.0 10^3	10.0	0.6
E_1	40.0 10^3	50.0	0.8

Table 7.1: Optimal development of the moduli of elasticity.

The optimal development of the reference viscosities are given by (4.12) and the parameters shown in Table 7.2.

	a (TPa hour)	b (hour^{-1})	c	d (hour^{-1})	e	f (hour)
η_1	67.5	0.004	0.4	5.0 10^{-9}	3.5	100.0
η_2	75.0	0.0045	0.6	5.0 10^{-9}	3.6	100.0

Table 7.2: Optimal development of the viscosities.

The optimal parameters governing the microprestress term are shown in Table 7.3.

S_0 (MPa)	c (hour^{-1})	a (MPa/°C)	k ((MPa)$^{-1}$/hour)
25.0	1.45	3.2	6.0 10^{-7}

Table 7.3: Optimal parameters for the microprestress term.

The maturity correction of the material parameters is carried out using an apparent activation energy for the hydration process of $U_{\text{hydration}} = 33.5$ kJ/mole. The diffusion correction is carried out using $U_{\text{diffusion}} = 16.0$ kJ/mole, which is equal to the activation energy for water.

7.3 Documentation of model with alternative concrete

Having obtained the material parameters for the alternative concrete as described above an experiment is carried out where a one-dimensional specimen is subjected to a prescribed strain history as shown in Fig. 7.3. The numerical analysis is similar to the one carried out for the documentation of the VD concrete parameters with the result shown in Fig. 6.18.

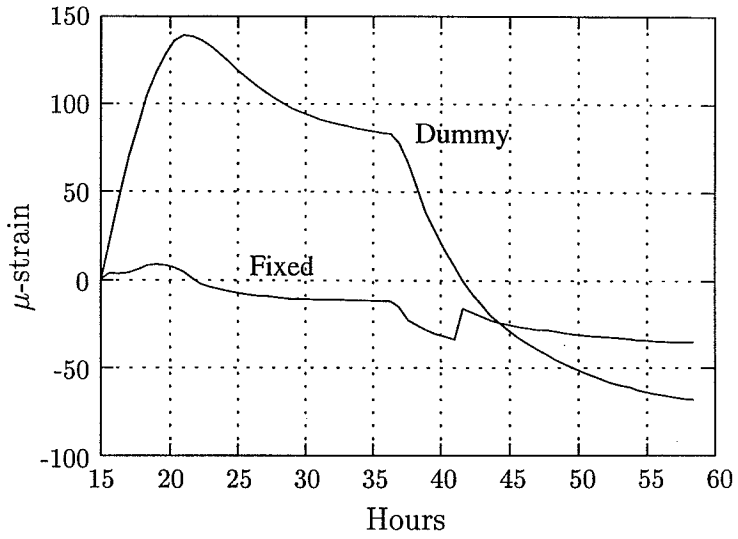

Figure 7.3: Loading on fixed specimen.

Fig. 7.3 shows the strain histories measured on the dummy and the fixed specimens and it is seen that the shrinkage and thermal deformations of the alternative concrete is 30% more than for the VD concrete. Again the difference between the two curves is used as load in the analysis of the fixed specimen and the measured temperature history shown in Fig. 7.4 is used for the corrections of the material parameters.

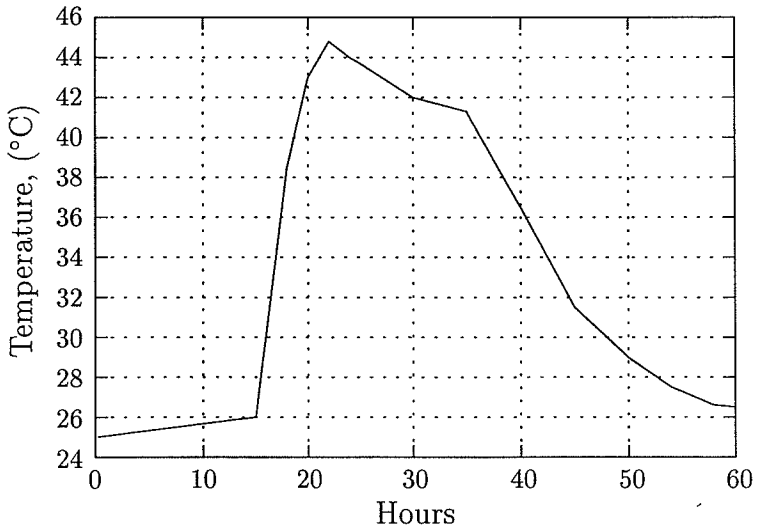

Figure 7.4: Temperature history.

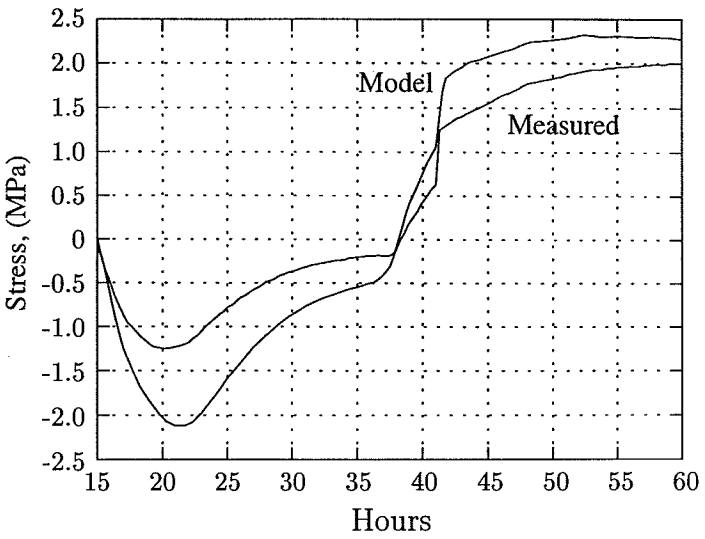

Figure 7.5: Experimental and numerical results.

Fig. 7.5 shows a comparison between the measured and numerical results. The overall agreement is acceptable and therefore it is concluded that sufficient information is obtained about the concrete with the experimental results mentioned above. In the comparison the uncertainties in the experimental results should be considered.

Chapter 8

Further Examples

Results from the litterature are analysed and they cover creep of early age concrete at different temperatures and creep of hardened concrete.

8.1 Creep at Different Temperature Levels

The measured creep at three different temperature levels reported in [55] has been used to study the influence from temperature on creep. The concrete was cured in sealed conditions at $20°C$ for the first 24 hours. The first specimen was loaded in compression and kept at $20°C$ whereas the others were loaded and heated to $40°C$ and $80°C$ respectively. The heating period has been estimated to 6 hours based on an analysis with temperature response diagrams. In this analysis typical heat and transport properties have been used corresponding to heating in an oven with circulating air. An unloaded companion specimen was used to compensate the loaded specimen for shrinkage and thermal deformations. The initial elastic strains were not reported so a reasonable value has been estimated and this is the same value for the three specimens since the initial curing is equal.

The results obtained with the model is shown in Fig. 8.1 and a large increase in creep strains with temperature is observed. Also shown are the results with and without including the microprestress term and it is seen that the microprestress term significantly improves the fits.

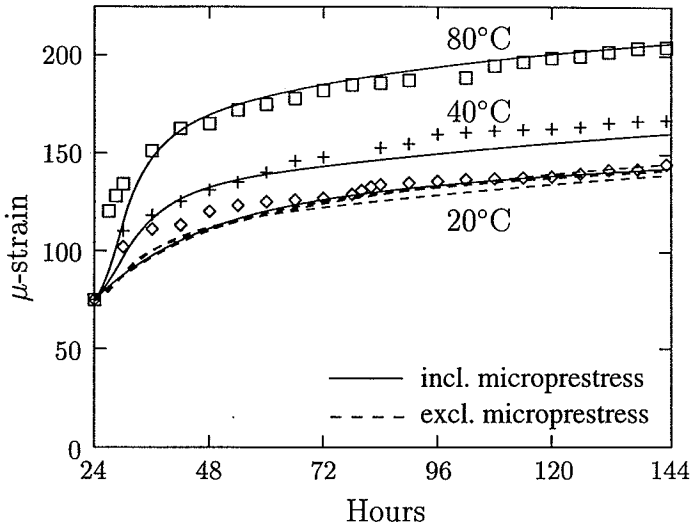

Figure 8.1: Fit of measured creep at different temperature levels.

The numerical model shows good agreement with the measured results particularly for the late response since the slopes are close. The initial creep at the highest temperature is a little off and this may be due to the simple modelling of the imbalance chosen. The optimal parameters are found to $a = 1.9$ MPa/°C, $k = 6.0\ 10^{-8}$ (MPa)$^{-1}$/hour, $c = 0.15$ hour and $S_0 = 1.0$ MPa. The resulting development of the imbalance is shown in Fig. 8.2.

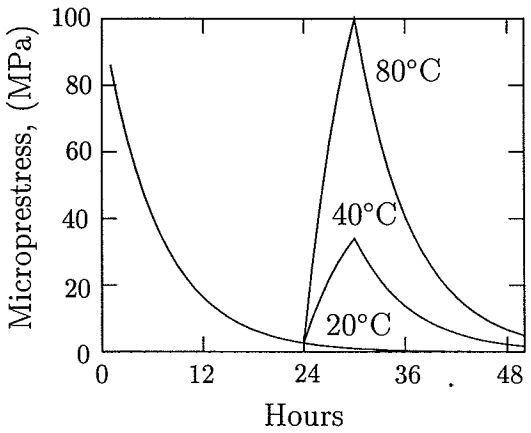

Figure 8.2: Development of imbalance.

The imbalance increases during the first 6 hours due to the temperature increase here and it is seen that the increase is largest for the heating to 80°C and afterwards the imbalance decreases exponentially. At 20°C no increase in imbalance is created and so the development levels off from the low initial value 1.0 MPa.

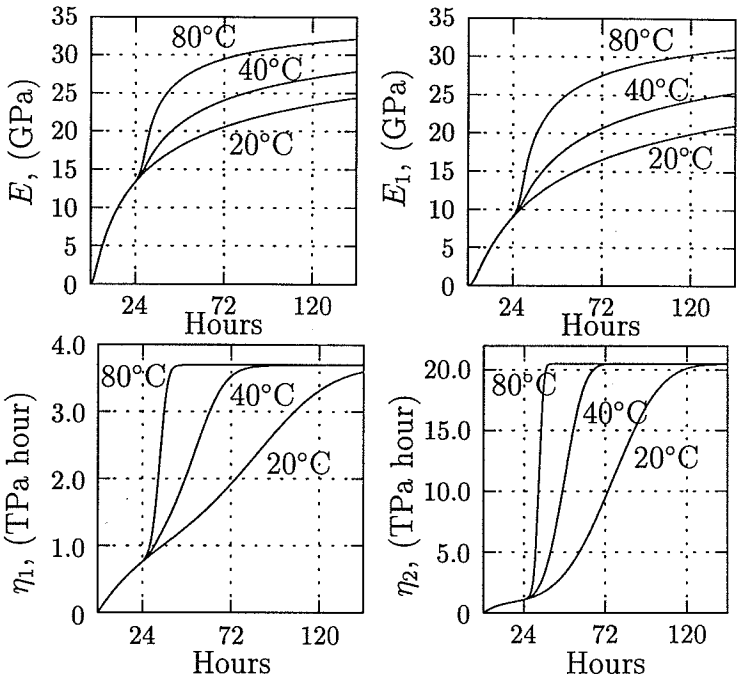

Figure 8.3: Development of properties after maturity correction.

The lower curves in Fig. 8.3 correspond to the $20°C$ development and the other curves correspond to 40 and $80°C$ respectively. In this maturity correction an activation energy of $U = 33.5$ kJ/mole has been used.

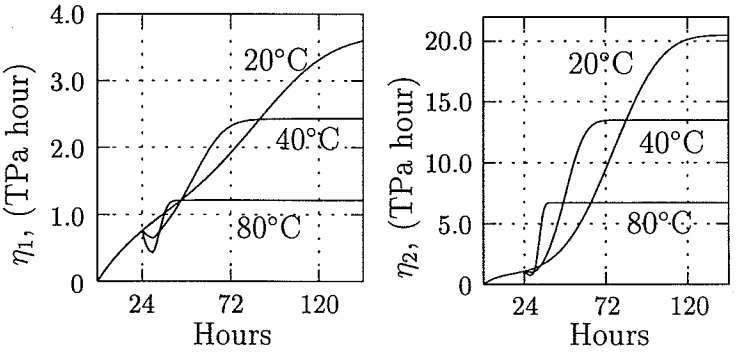

Figure 8.4: Development of viscosities after diffusion correction.

The final viscosities used in the fitting of the data are obtained by scaling the viscosities in Fig. 8.3 with a temperature dependent factor and the result is shown in Fig. 8.4. The activation energy used in this last scaling is $U_{diffusion} = 16.0$ kJ/mole and this correspond to the value found in [49] for cement paste.

8.2 Creep of Hardened Concrete

Concrete for which the hydration process has ceased does also exhibit creep properties and to show that the proposed model handles this case, two examples from the litterature have been analysed.

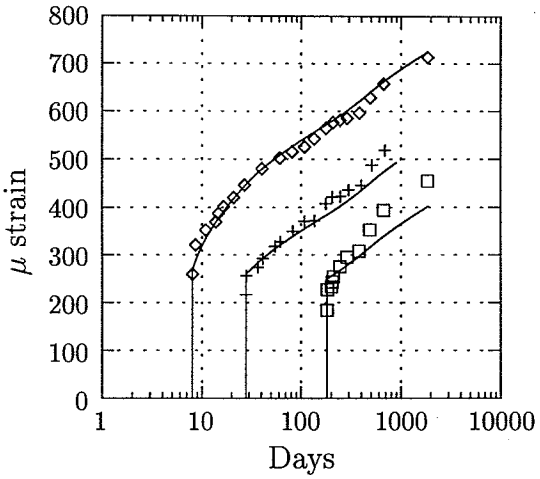

Figure 8.5: Fit of creep of hardened concrete. Experiments form [12]. Fitting with the model presented here.

The first example deals with creep of concrete loaded in compression at the ages 8, 28 and 182 days respectively, [12]. The specimens are sealed throughout the complete test period with a duration of about 2000 days and the temperature is kept constant. Fig. 8.5 shows the measured creep and the results of the numerical modelling.

Since no hardening is assumed to take place only the two parameters, an elastic modulus and a viscosity, shown in Fig. 8.6 have been used. The elastic modulus is slightly increasing and the viscosity increases with time.

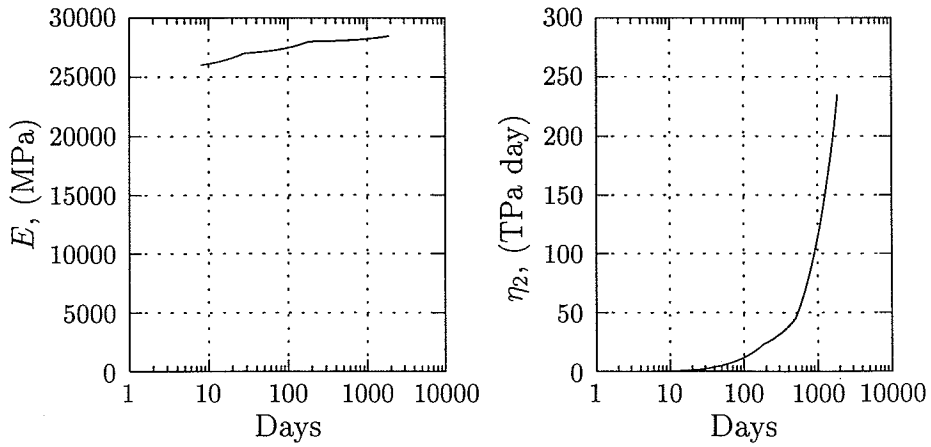

Figure 8.6: Material parameters used in the fitting of the results in Fig. 8.5.

Further the second example also deals with creep in compression and here the ages at

loading were 7, 28 and 365 days respectively, [34]. The curing conditions are again sealed and a constant temperature. The result is shown in Fig. 8.7.

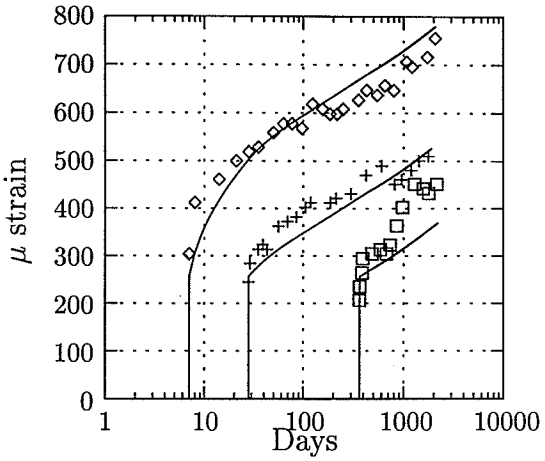

Figure 8.7: Fit of creep of hardened concrete. Experimental results from [34].

In the examples shown here for hardened concrete there are some discrepancy between the measured creep and the numerical results. The reason for this is two-fold and firstly the model used is very simple consisting of only two elements and secondly the test conditions are assumed constant which is hard to fulfill for several years in a laboratory.

8.3 Redistribution of Stresses

The final example is 2-dimensional and illustrates redistribution of stresses due to creep. The model has been implemented in a finite element program and the tall beam shown in Fig. 8.8 has been analysed. This example is numerical since no experimental data has been available. As shown the beam is subjected to a bending moment in the free end and completely fixed in the other end.

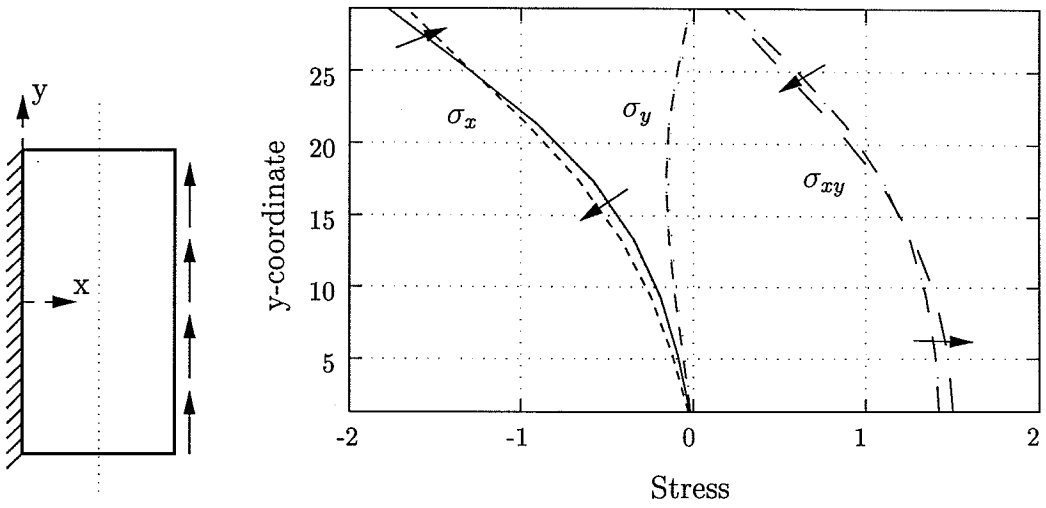

Figure 8.8: The analysed tall beam and stress distributions initially and after long time.

The stress distributions along the dotted line for the upper half of the structure are also shown in Fig. 8.8 together with their development in time indicated by the arrows. The creep model consists of an initial spring and one Kelvin cell and the parameters are constants. Shear creep deformations are decoupled by choosing the viscosity matrix

$$\boldsymbol{\eta} = \begin{bmatrix} 10.0 & 3.0 & 0.0 \\ 3.0 & 10.0 & 0.0 \\ 0.0 & 0.0 & \infty \end{bmatrix} \tag{8.1}$$

Due to creep the stiffness in the x-direction decreases and this means that the peak normal stresses, σ_x, in the outer fiber of the beam decreases with time as seen whereas the shear stresses, σ_{xy}, increases. The decrease in peak normal stresses is accompanied by an increase in normal stresses closer to the centerline of the beam since the same moment need to be carried.

Chapter 9

Conclusion

In this report the concepts of material modelling have been discussed and here a separation between the total models and the incremental models is made. In the total formulations knowledge about the complete loading history is needed at every instant in the analysis. In an incremental form the loading history is summed up in certain memory variables thus avoiding the storage. The basis chosen in the present context is the incremental form and the concrete is treated as a continuum.

The development of the properties at early age is the result of chemical reactions termed the hydration process. Several factors influence the progress of hydration such as the development of temperature and the development of the moisture distribution. The factors are coupled and numerical analysis taking into consideration the couplings is discussed. A material model is proposed which include some of the couplings and it is shown how more may be incorporated. Particularly the coupling between temperature and creep is studied. The model is illustrated through analysis of measured creep response both at a varying load history and at a varying temperature history.

From the experiments carried out in another subtask of the HETEK project it has been found that the temperature significantly influences the creep properties at early age. It is shown here how this influence may be incorporated in the numerical model using the Arrhenius principle and the concept of microstresses. The microstresses are large local stresses in the microstructure of the concrete and temperature and humidity variations significantly influences the development of these stresses. Following this scheme is an attempt to relate the development of the material properties to the physical processes taking place in the concrete at early age. To formulate a detailed standard test program more information about these phenomena are needed.

The additional material parameters needed to describe the temperature influence may be found from a few compressive tests of creep at a variable temperature. Further, the analysis of the tensile creep measurements show that creep in tension is of the same order of magnitude as creep in compression at load levels below about 60%. At higher load levels, we tested only at 80%, some non-linearities were observed.

The necessary material parameters for characterisation of the influence from temperature on the creep properties may be characterised from measurements in compression. To get an idea about the non-linearity observed in tension some tensile experiments at a high load

level are needed. The tensile properties at lower stress levels may be obtained from the compressive experiments.

The proposed model is checked by means of a fixed specimen subjected to temperature and shrinkage load. The stress history was measured and compared with the numerical results and an acceptable accuracy was obtained for two different concrete mixes.

Chapter 10

Current Practice

10.1 DTI Test Method: TI-B 102

As shown in Fig. 10.1 both permanent and reversible strains are seen when a test specimen is loaded and unloaded. It should be noted that the presented strains are pure creep strain without any contribution from elastic strains due to loading/unloading.

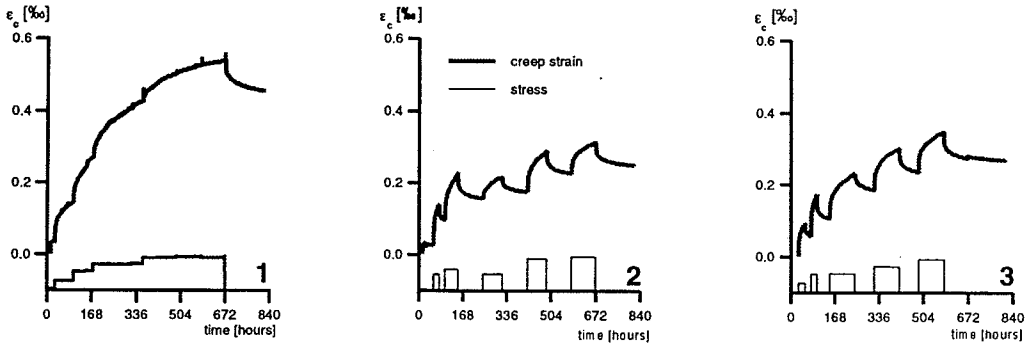

Figure 10.1: Measured creep strains. It should be noted that the presented strains are pure creep strain without any contribution from elastic strains due to loading/unloading.

A creep model as shown in Fig. 10.2 is well suited to describe such a progress of creep strains. Permanent and reversibel parts of the creep strains are described by the single dashpot and the parallel coupling respectively.

In order to obtain information about creep properties during the whole hardening process three load histories are prescribed in the test method TI-B 102, [54].

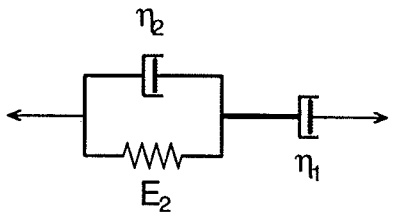

Figure 10.2: Creep model describing pure creep strains.

By means of the least square method the developments of the properties for the spring and dashpots, which give the best agreement between observations and creep model, can be formed.

The development of the properties used in practice are

$$f(M) = a\exp(bM) \tag{10.1}$$

or

$$f(M) = a + b\exp(-\left(\frac{c}{M}\right)^d) \tag{10.2}$$

where f is the actual property and a, b, c and d are positive constants. The constants are determined by the former mentioned least square method or simply by an educated guess.

The mathematical model recommended in TI-B 102 differ from the proposed creep model described in Chapter 4. The difference lies in the calculation of the stress in the spring. TI-B 102:

$$\sigma_{\text{spring}}(t_i) = \varepsilon(t_i)E(t_i) \tag{10.3}$$

and Chapter 4:

$$\sigma_{\text{spring}}(t_i) = \Delta\varepsilon(t_1)E(t_1) + \cdots + \Delta\varepsilon(t_i)E(t_i) \tag{10.4}$$

The formulation in TI-B 102 leads to reversible strains in the parallel coupling and permanent strains in the single dashpot. In the model described in Chapter 4 permanent strains are build up in both the parallel coupling and the single dashpot. Further the model from Chapter 4 uses the current value of the modulus of elasticity to relate the stress increments to the strain increments as shown in (10.4), and thereby the material model reflects the hydration process where new layers of cement gel are formed in a stress free state.

Due to the difference in the models different properties for the spring and dashpots will be found when the same test results are fitted. The development of the properties for the parallel coupling are almost identical but the viscosity for the dashpot are higher in the proposed model from Chapter 4 because permanent creep also is generated in the parallel coupling. The Finite Element programs CIMS-2D, [15], and Fiesta, [22], use the model described in TI-B 102.

Bibliography

[1] Adamson, Arthur W., (1990). *Physical Chemistry of Surfaces* 5.th. edition, John Wiley & Sons, New York.

[2] Andersen, M.E., (1995). *Design and Construction of Concrete Structures in View of Early-Age Thermal Effects.* Industrial Research Education, Ph.D, EF406, G.M. Idorn Consult, Rambøll. Department of Structural Engineering, Technical University of Denmark.

[3] Arthanari, S. and Yu, C.W. (1967). *Creep of concrete under uniaxial and biaxial stresses at elevated temperatures*, Magazine of Concrete Research, Vol. 19, No. 60.

[4] Bažant, Z.P., ed. (1970). *Constitutive equation for concrete creep and shrinkage based on thermodynamics of multiphase systems*, Materials and Structures, Vol. 3, No. 13.

[5] Bažant, Z.P., ed. (1972). *Thermodynamics of Interacting Continua with Surfaces and Creep Analysis of Concrete Structures*, Nuclear Engineering and Design, Vol. 20, pp. 477–505.

[6] Bažant, Z.P., ed. (1988). *Mathematical modeling of creep and shrinkage of concrete.* John Wiley, New York, N.Y.

[7] Bažant, Z.P. and Najjar, L.J. (1972). *Nonlinear water diffusion in nonsaturated concrete*, Materials and Structures, Vol. 5, No. 25.

[8] Bažant, Z.P. and Osman, E., (1975). *Double power law for basic creep of concrete*, Materials and Structures, Vol. 9, No. 49.

[9] Bažant, Z.P., Hauggaard, A.B., Baweja, S. and Ulm, F.-J., (1996). *Microprestress-Solidification Theory for Aging and Drying Effects on Concrete Creep*, accepted for publication in Journal of Engineering Mechanics.

[10] Bell, K. ed. (1994). *NSCM VII, Seventh Nordic Seminar on Computational Mechanics*, Department of Structural Engineering, The Norwegian Institute of Technology, Trondheim, Norway.

[11] de Borst, R. and van den Boogaard, A.H. (1995). *Finite-Element Modeling of Deformation and Cracking in Early-Age Concrete.* Journal of Engineering Mechanics, Vol. 120, No. 12, pp. 2519–2534.

[12] Bryant, A.H. and Vadhanavikkit, C., (1987). *Creep, Shrinkage-Size, and Age at Loading Effects*, ACI Materials Journal, pp. 117–123.

[13] Byfors, J. (1980). *Plain Concrete at Early Ages*, CBI Forskning, Research 3:80, Swedish Council for Building Research.

[14] Carlson, R.W. (1937). *Drying Shrinkage of Large Concrete Members*, Proceedings of the American Concrete Institute, Vol. 33, pp. 327–336.

[15] CIMS-2D manual (1994). DTI, Byggeteknisk Institut.

[16] COSMOS manual (1993). Version 1.70.

[17] Emborg, M., (1989). *Thermal stresses in concrete structures at early ages*, Doctoral Thesis, Division of Structural Engineering, Luleå University of Technology.

[18] Freiesleben Hansen, P. (1978). *Hærdeteknologi, 1: Portlandcement og 2: Dekrementmetoden*, Aalborg Portland og BKF-Centralen.

[19] Freiesleben Hansen, P. (1995). *Materialefysik for Bygningsingeniører*, SBI-Anvisning 183, Statens Byggeforskningsinstitut.

[20] Freiesleben Hansen, P. og Petersen, E.J., (1977). *Måleinstrument til kontrol af betons hærdning,* Nordisk Betong.

[21] Germann Instruments, In-situ Test Systems, Fast Track Construction with COMA-Meter maturity testing, ASTM C 1074 and LOK-TEST pullout testing, ASTM C 900. 1994.

[22] Grodtkjær, E. (1987). *Beregning af spændinger i hærdnende betonkonstruktioner*, Dansk Beton, Nr. 3.

[23] Grzybowski, M., (1993). *Measurement system for evaluation of cracking risks due to temperature differences and creep*, in Swedish, Royal Institute of Technology, Department of Structural Engineering, Stockholm, Sweden.

[24] Gutsch, A. and Rostásy, F.S., (1994). *Toung concrete under high tensile stresses - creep, relaxation and cracking*, Proc. of the RILEM Symposium on Thermal Cracking in Concrete at Early Ages, Münich, Ed. R. Springenschmid.

[25] Hansen, T.C. (1960). *Creep and Stress Relaxation of Concrete*, Swedish Cement and Concrete Research Institute, Stockholm.

[26] Hauggaard, A.B., Damkilde, L., Freiesleben Hansen, P., Hougaard Hansen, J. and Nielsen, A., *HETEK, Control of Early Age Cracking in Concrete, Phase 3: Creep in Concrete*, Report No. xx, The Danish Road Directorate.

[27] Hauggaard-Nielsen, A.B. (1997). *Numerical Modelling of Early Age Concrete*, PhD-thesis, to be published.

[28] Hedlund, H., (1996). *Stresses in High Performance Concrete due to Temperature and Moisture Variations at Early Ages*, tech. lic., Luleå Institute of Technology, Luleå, Sweden.

[29] Herholdt, AA.D., Justesen, Chr. F.P., Nepper-Christensen, P. og Nielsen, A., (1985). *The Concrete bool*, in danish, 2. ed., The technical information center of the cement-producers, Aalborg, Denmark.

[30] Hillerborg, A., Modeer, M. and Petersson, P.-E. (1976). *Analysis of Crack Formation and Crack Growth in Concrete by Means of Fracture Mechanics and Finite Elements* Cement and Concrete Research, Vol. 6, pp. 773–782.

[31] Jensen, O.M. (1993). *Autogeneous deformation and RH-changes – Selfdesiccation and selfdesiccation shrinkage*, in danish, Building Materials Laboratory, Technical University of Denmark, Copenhagen Denmark, Report number TR 284/93, ISSN 0907-7073.

[32] Jensen, O.M., et al., (1996). *HETEK, Control of Early Age Cracking in Concrete, Phase 2: Shrinkage of Concrete*, Report No. xx, The Danish Road Directorate.

[33] Kasai, Y., Yokoyama, K. and Matsui, I., (1972). *Tensile Properties of Early-Age Concrete*, Proceedings of the international conference on mechanical behavior of materials, Vol. 4, p. 288, The society of materials science, Japan.

[34] L'Hermite, R., Mamillan, M. and Lefèvre, C. (1965). *Nouveaux Rèsultats de Recherches sur la Dèformation et la Rupture du Bèton*, Annales de L'Institut Technique du Batiment et des Travaux Publics, No. 207–208.

[35] Li, V.C., Stang, H. and Krenchel, H. (1993) *Micromechanics of crack bridging in fibre-reinforced concrete* Materials and Structures, Vol. 26, pp. 486–494.

[36] LUSAS manual (1990). Finite Element System, version 10.0, Theory manual.

[37] Mehta, P.K., and Monteiro, P.J.M., (1993). *Concrete, Structure, Properties and Materials*, Prentice Hall, Englewood Cliffs, 2. ed.

[38] Neville, A.M., Dilger, W.H. og Brooks, J.J. (1983). *Creep of plain and structural concrete*, Construction Press, London and New York.

[39] Nielsen, A. (1972). *Rheology of Building Materials*, National Swedish Building Research, Document D6.

[40] Nielsen, L.F., (1980). *On the prediction of rheological parameters for concrete*, Nordic Seminar on Deformations in Concrete Structures, Copenhagen, pp. 81–118, Proc. edited by Gunnar Mohr, DIALOG 1–80, Danish Engineering Academy, Copenhagen.

[41] Mjörnell, K.N., (1994). *Self-desiccation in concrete*, Report P-94:2, Chalmers University of Technology.

[42] Pedersen, E.S., Olsen, S.Ø. og Lykke, S. (1995). *Curing Technology on the Øresund Link basis for Stress Calculations* Proceedings of the Nordic Symposium on Modern Design of Concrete Structures.

[43] Pickett, G. (1942). *The Effect of Change in Moisture-Content of the Creep of Concrete Under a Sustained Load*, Proceedings of the American Concrete Institute, Vol. 38, No. 4.

[44] Pickett, G. (1946). *Shrinkage Stresses in Concrete*, Proceedings of the American Concrete Institute, Vol. 17, No. 3 and 4.

[45] Powers, T.C., and Brownyard, T.L., (1946-47). *Studies of the Physical Properties of Hardened Portland Cement Paste*, nine parts, Journal of the American Concrete Institute, Vol. 18, No. 2–8.

[46] Powers, T.C., (1968). "The Thermodynamics of volume change and creep." *Matériaux et Constructions,*, 1(6).

[47] Rüsch, H. (1960). *Researches toward a general flexural theory for structural concrete* Proceedings for the American Concrete Institute, Vol. 57, No. 1, pp. 1–28.

[48] Schaumann, J. (1995) *Reaktionskinetik og temperatureffekt i portlandcement systemer med microsilica og flyveaske*, Aalborg Universitet, Instituttet for Bygningsteknik, Materialelære, PhD-rapport.

[49] Sellevold, E.J. and Richards, C.W., (1972). *Short-Time Creep Transition for Hardened Cement Paste*, Journal of the American Ceramic Society, Vol. 55, No. 6.

[50] Sereda, P.J., Feldman, R.F. and Swenson, E.G., (1966). *Effect of Sorbed Water on Some Mechanical Properties of Hydrated Portland Cement Pastes and Compacts*, Highway Research Board, Special Report, No. 90, pp. 58–73.

[51] Soroka, I., (1979). *Portland Cement Paste and Concrete*, The Macmillan Press Ltd.

[52] Spange, H. and Pedersen, E.S., (1996). *HETEK, Control of Early Age Cracking in Concrete, Phase 1: Early Age Properties of Selected Concrete*, Report No. xx, The Danish Road Directorate.

[53] Riis, K. and Spange, H., (1997). *HETEK, Control of Early Age Cracking in Concrete, Phase 6: Early Age Properties of Alternative Concrete*, Report No. xx, The Danish Road Directorate.

[54] TI-B 102, *Test Method Concrete Strains from Creep and Early-Age Shrinkage*, Version 1, Sept. 1994, The Concrete Center, DTI Building Technology.

[55] Umehara, H., Uehara, T., Iisaka, T. and Sugiyama, A., (1994). *Effect of creep in concrete at early ages on thermal stress*, Proc. of the RILEM Symposium on Thermal Cracking in Concrete at Early Ages, Münich, Ed. R. Springenschmid.

[56] Vattenfall Vattenkraft, (1992). *Hacon-S A Program for Simulation of Stress in Hardening Concrete*, Program developed by Dahlblom, O., Lund Institute of Technology, Sweden.

[57] Brophy, J.H., Rose, R.M. and Wulff, J.,(1964). *Thermodynamics of Structure*, Structure and Properties of Materials, vol. II, Wiley & Sons.

[58] The standard for concrete structures, The danish association of engineers, in Danish, DS 411, 3. ed., (1984), Copenhagen, Denmark.